

Transcriptome-wide N⁶-methyladenosine profiling of rice responding to brown planthopper (*Nilaparvata lugens*) infestation reveals growth–defense trade-offs

Shuai Li¹, Xinyang Tan¹, Zhen He², Lei Jiang³, Yali Li⁴, Liu Yang⁴, Ary A. Hoffmann⁵, Chunqing Zhao⁶, Jichao Fang¹, and Rui Ji¹

¹Jiangsu Academy of Agricultural Sciences

²Yangzhou University College of Plant Protection

³Anhui Agricultural University

⁴Wuhan Benagen Technology Company Limited

⁵The University of Melbourne School of BioSciences

⁶Nanjing Agricultural University College of Plant Protection

November 20, 2023

Abstract

N⁶-methyladenosine (m⁶A) is a common messenger RNA (mRNA) modification that affects diverse physiological processes in stress responses. However, the role of m⁶A modification in plants coping with herbivore stress remains unclear. Here we found that an infestation of brown planthopper (BPH) *Nilaparvata lugens* female adults enhanced the rice resistance to BPH. An m⁶A methylome analysis of BPH-infested and un-infested rice samples were measured to explore the interaction between rice and BPH. m⁶A methylation occurs mainly in genes actively expressed in rice following BPH infestation, while an analysis of the whole-genomic mRNA distribution of m⁶A showed that BPH infestation caused an overall decrease in the number of m⁶A methylation sites across the chromosomes. Genes involved in components of the m⁶A modification machinery, BPH resistance, and several defense-related (such as JA, SA and cellulose) pathways were heavily methylated by m⁶A in BPH-infested rice compared to those in un-infested rice. In contrast, m⁶A modification levels of growth-related phytohormones (auxin and gibberellin) biosynthesis-related genes were significantly attenuated under BPH attack, accompanied by downregulated expression of these transcripts, indicating that rice growth was restricted during BPH attack to rapidly optimize resource allocation for plant defense. Integrative analysis of the differential patterns of m⁶A methylation and the corresponding transcripts showed a positive correlation between m⁶A methylation and transcriptional regulation. In conclusion, the process of m⁶A modification acts as an important strategy for regulating expression of genes involved in rice defense and growth during rice-BPH interaction.

Transcriptome-wide N⁶-methyladenosine profiling of rice responding to brown planthopper (*Nilaparvata lugens*)

infestation reveals growth–defense trade-offs

Shuai Li¹, Xinyang Tan^{1,2}, Zhen He⁴, Lei Jiang⁵, Yali Li⁷, Liu Yang⁷, Ary A. Hoffmann⁶, Chunqing Zhao², Jichao Fang^{1,2}, Rui Ji^{1,3}

¹ Institute of Plant Protection, Jiangsu Academy of Agricultural Sciences, Jiangsu Key Laboratory for Food and Safety-State Key Laboratory Cultivation Base of Ministry of Science and Technology, Nanjing 210014, China

² College of Plant Protection, Nanjing Agricultural University, Nanjing 210095, China

³ School of Life Sciences, Anhui Normal University/Key Laboratory for Conservation and Use of Important Biological Resources of Anhui Province, Anhui 241000, China

⁴ School of Plant Protection, Yangzhou University, Yangzhou 225009, China

⁵ School of Plant Protection, Anhui Agricultural University, Hefei 230000, China

⁶ School of BioSciences, Bio21 Institute, University of Melbourne, Parkville, VIC 3010, Australia

⁷ Wuhan Benagen Technology Company Limited, Wuhan 430000, China

Shuai Li and Xinyang Tan contributed equally to this work.

Correspondence:

Jichao Fang and Rui Ji, Institute of Plant Protection, Jiangsu Academy of Agricultural Sciences, Jiangsu Key Laboratory for Food and Safety-State Key Laboratory Cultivation Base of Ministry of Science and Technology, 210014 Nanjing, China.

Email: fangjc@jaas.ac.cn (J. F.) and jirui@jaas.ac.cn (R. J.).

Funding information

National Natural Science Foundation of China/Award number: 32302320; Jiangsu Agricultural Science and Technology Independent Innovation Fund/Award number: CX(22)3018; National Key Basic Research Program of China/Award number: 2021YFD1401100.

Abstract

*N*⁶-methyladenosine (m⁶A) is a common messenger RNA (mRNA) modification that affects diverse physiological processes in stress responses. However, the role of m⁶A modification in plants coping with herbivore stress remains unclear. Here we found that an infestation of brown planthopper (BPH) *Nilaparvata lugens* female adults enhanced the rice resistance to BPH. An m⁶A methylome analysis of BPH-infested and un-infested rice samples were measured to explore the interaction between rice and BPH. m⁶A methylation occurs mainly in genes actively expressed in rice following BPH infestation, while an analysis of the whole-genomic mRNA distribution of m⁶A showed that BPH infestation caused an overall decrease in the number of m⁶A methylation sites across the chromosomes. Genes involved in components of the m⁶A modification machinery, BPH resistance, and several defense-related (such as JA, SA and cellulose) pathways were heavily methylated by m⁶A in BPH-infested rice compared to those in un-infested rice. In contrast, m⁶A modification levels of growth-related phytohormones (auxin and gibberellin) biosynthesis-related genes were significantly attenuated under BPH attack, accompanied by downregulated expression of these transcripts, indicating that rice growth was restricted during BPH attack to rapidly optimize resource allocation for plant defense. Integrative analysis of the differential patterns of m⁶A methylation and the corresponding transcripts showed a positive correlation between m⁶A methylation and transcriptional regulation. In conclusion, the process of m⁶A modification acts as an important strategy for regulating expression of genes involved in rice defense and growth during rice-BPH interaction.

KEYWORDS

rice *N*⁶-methyladenosine, brown planthopper, plant defensive pathways, plant growth, gene regulation

1 INTRODUCTION

Over 200 distinct RNA modifications have been discovered in eukaryotes, of which RNA methylation is a critical post-transcriptional modification that affects gene expression. Among these, the most important and well-studied modification is *N*⁶-methyladenosine RNA methylation (m⁶A) (Shinde et al., 2023), which refers to the insertion of a methyl substituent on the 6th position *N*-atom in messenger RNA (mRNA) adenosine (Wei et al., 2018). This occurs widely in eukaryotes such as yeast, fruit flies, plants, and animals (Dominissini

et al., 2012) and is the most abundant form of methylation in eukaryotic mRNA and various non-coding RNAs. It controls the fate of RNA at different levels of genetic information transmission, including RNA synthesis and processing, mRNA stability, and translation (Liu et al., 2020b). The m⁶A modification exerts regulatory functions during RNA synthesis and splicing, influencing the transcription rate, gene stability, and RNA splicing selection. m⁶A-modified RNA molecules are more prone to recognition and degradation by RNA degradation enzymes. This regulates RNA lifespan and clears abnormal RNA molecules, thus maintaining the dynamic RNA equilibrium within a cell (Sekula et al., 2020). m⁶A plays a key role in regulating transcription and translation efficiency, thereby controlling the speed of protein synthesis (Bodi et al., 2012; Liu et al., 2020b).

m⁶A is a reversible chemical modification in which a methyl group is provided by “DONOR,” catalyzed by “WRITER,” removed by “ERASER,” and recognized by the m⁶A-binding protein “READER” (Shinde et al., 2023). S-adenosylmethionine (SAM) serves as the methyl “DONOR” for almost all cellular methylation reactions (Shen et al., 2016a). “WRITER” is a high-molecular-weight RNA methyltransferase complex capable of writing m⁶A modifications into mRNA. “ERASER” is usually affected by demethylases; ALKBH9B and ALKBH10B are well-known demethylation proteins in *Arabidopsis* which can remove m⁶A from single-stranded RNA of alfalfa mosaic virus (Martínez-Pérez et al., 2017) and *Arabidopsis* (Duan et al., 2017) *in vitro*, respectively. The main function of m⁶A modification depends on its “READER” proteins. In plants, research on m⁶A “READER” proteins is primarily focused on YTH domain proteins; 13 such proteins have been detected in *Arabidopsis*, all of which can bind to the m⁶A position (Wang et al., 2015).

Emergence of various high-throughput sequencing techniques targeting m⁶A has facilitated functional studies on this RNA modification. These methods include antibody-dependent m⁶A sequencing and nanopore direct RNA sequencing (DRS) (Wang et al., 2020; Bertheliet et al., 2023). Nanopore DRS is a powerful approach that bypasses reverse transcription, requires no amplification, and does not exhibit sequencing bias (Pratanwanich et al., 2021). It can simultaneously detect methylation modification sites on RNA, accurately analyze alternative splicing, and identify novel isoforms (Bertheliet et al., 2023). m⁶A sites are primarily enriched around termination codons and within 3'-untranslated regions (3'-UTRs), exhibiting the m⁶A consensus motif “RRACH” (R=A/G; H= A/C/U) (Parker et al., 2020). These findings have provided strong evidence for a conserved mechanism of m⁶A deposition in eukaryotic mRNA.

m⁶A methylation plays a crucial role in modulating gene expression and biological process in eukaryotes (Wei et al., 2018; Song et al., 2023). In mammalian, different mechanisms of RNA m⁶A modification in cancer and their potential correlation with cancer prognosis have been elucidated (Wang et al., 2023c). In insects, m⁶A methylation plays key roles in sex determination, neuronal function, and development (Wang et al., 2021; Chen et al., 2023). Moreover, m⁶A modification has profound implications in the regulation of pathogen and insecticide resistance. The 5'-UTR of cytochrome P450 gene (*CYP4C64*) in the insecticide-resistant *Bemisia tabaci* has a m⁶A mutant site, thus the gene can't be m⁶A methylated, thereby increasing gene expression, and enhancing *B. tabaci* resistance to thiamethoxam (Yang et al., 2021). In plants, m⁶A modification plays a regulatory role in vegetative growth, floral transition, reproductive development, fruit ripening, photomorphogenesis, and the circadian clock (Tang et al., 2023). m⁶A also mediates salt tolerance by regulating ROS homeostasis, and auxin signaling in a tissue-specific manner (Wang et al., 2022). In addition, m⁶A methylation is increased in rice infected with rice stripe virus (RSV) or rice black-stripe dwarf virus (RBSDV), several antiviral pathway-related genes—such as RNA silencing, resistance, and fundamental antiviral phytohormone metabolism-related genes—are methylated by m⁶A (Zhang et al., 2021a). m⁶A modification might be an epigenetic mechanism that regulates RBSDV replication in small brown planthoppers (SBPH) and maintains a certain viral threshold required for persistent transmission (Tian et al., 2021). Thus, the modification of m⁶A in plants may also play an important role in regulating plant defense against insect, but this has rarely been explored to date.

When attacked by herbivores, plants activate early signaling events, such as mitogen-activated protein kinases (MAPKs). Then the production of defense-related phytohormones, such as jasmonic acid (JA) and salicylic acid (SA), are induced, which are well known to regulate the production of defensive compounds

and thus confer resistance to (Erb et al., 2019). The brown planthopper (BPH; *Nilaparvata lugens* Stal) is a monophagous sap-sucking herbivore that causes severe yield reductions and economic losses in rice crops (Otuka, 2013). It causes direct damage to rice plants by feeding on phloem sap via its ovipositor and laying egg clusters in tissues (Bass et al., 2011). The JA upregulates sakuranetin synthesis in rice and enhances resistance against BPH (Liu et al., 2023). While SA mediates the accumulation of anti-insect callose in the phloem (Wang et al., 2023b). To date, numerous BPH resistance genes (*Bphs*) have been well-documented in rice. Among them, several *Bphs* regulate phytohormones signaling pathways and exhibit various mechanisms of insect resistance (Hu et al., 2011; Li et al., 2023; Pannak et al., 2023). Bph14 activates SA-mediated callose deposition in rice leaf sheath and exhibits BPH resistance in early stage rice seedlings (Du et al., 2009). For BPH, successful phloem feeding is achieved by penetrating the sclerenchyma tissue of the rice epidermis using its stylet (Shi et al., 2021). The sclerenchyma tissue is mainly composed of cellulose, hemicellulose, and lignin, providing mechanical strength and stability to rice stems. *Bph30* and *Bph40* were highly expressed in sclerenchyma cells and enhanced cellulose and hemicellulose synthesis, which makes the cell walls stiffer and sclerenchyma thicker and thus enhance resistance to BPH by inhibiting insect feeding (Shi et al., 2021). Upon BPH infestation, rice defense is activated but growth is suppressed (Jin et al., 2023). The crosstalk of defense- and growth-related phytohormones plays an important role in the growth–defense trade-offs (Li et al., 2015). JA signaling activates defense responses and plays a central role in prioritizing defense over growth during herbivore attacks, by suppressing growth-related phytohormones pathways, such as auxin and GA (Hou et al., 2010; Chen et al., 2011; Yang et al., 2012; Jin et al., 2023).

Using nanopore DRS approach combined with RNA sequencing, we aimed to examine the interactions between rice and BPH by investigating the dynamic modulation of m⁶A modification in rice genome. We identified the specific genes and pathways that are influenced by these modifications, to deepen our understanding of how m⁶A modifications contribute to rice defenses against BPH at the expense of plant growth.

2 MATERIALS AND METHODS

2.1 Plant growth and insect rearing

Oryza sativa L. japonica. cv. Nipponbare rice was used in this study. The rice seeds were planted into a 600 mL plastic pot filled with sterile soil under controlled conditions, with a temperature maintained at 28 ± 2degC and a 16 hours (h)/8 h light-dark cycle (Hasan et al., 2022). After 40 days, these rice plants were subjected to infestation by gravid BPH female adults. The colonies of BPH were collected from rice fields in Nanjing, China, and were reared on rice seedlings in a climate chamber under a constant temperature of 28 ± 1 and a 16 h/8 h light/dark cycle.

2.2 BPH Bioassays

The choice test was conducted as follows (Li et al., 2023): two rice plants were potted side-by-side in the same plastic container, and each plant was placed in glass cylinders (2 cm diameter x 8 cm height), which surrounded the basal stem of each plant. One was infested with 20 gravid BPH female adults, and the other was used as an un-infected control. After 24 hours of infestation, BPHs were removed and one pair of plants was confined in a glass cylinder (4 cm diameter x 8 cm height) into which 15 fifth-instar nymphs or gravid BPH female adults were released in the middle of the two plants. Afterwards, BPHs settling on each plant were counted at 2, 4, 8, 12, 24, and 48 hours, respectively. The experiment was repeated 12 times with 15 insects per replicate.

In the survival rate and honeydew measurement tests, the gravid BPH females pre-infested and control plants were prepared using the same method as above. Third-instar BPH nymphs were allowed to feed on rice plants, stems of rice plants (one plant per pot) were confined individually within glass cylinders, into which 15 third-instar BPH nymphs were released (Ji et al., 2017). The number of surviving BPH nymphs in each cylinder was recorded every day. The experiment was repeated four times. The honeydew was measured as follows (Ji et al., 2021): a brachypterous newly emerged BPH female adult was placed into a small Parafilm bag (6x5 cm), which was then fixed on the stem of a rice plant. The amount of honeydew excreted by a female adult was weighed (to an accuracy of 0.1 mg) at 24 hours after the start of the experiment. The

experiment was replicated 18 times.

2.3 Plant treatment with BPH

Rice seedlings were placed in a 600 mL plastic pot, and cotton pads were placed at the base of each rice stem to prevent BPH from burrowing into the nutrient soil (Supporting Information: Figure S1). The differentially expressed genes (DEGs) were significantly enriched in the rice hormone signaling pathway after 8 h of sustained BPH attack, compared with other time intervals (Xu et al., 2021). This was also reflected in the hierarchical cluster analysis of DEGs between BPH-infested (NI-Nip_1, NI-Nip_2) and un-infested control (Nip_1, Nip_2) groups (Supporting Information: Figure S2). Therefore, samples used for library construction were collected from Nip or NI-Nip rice leaf sheaths after 8 h of continuous feeding by 20 BPH female adults (Zha et al., 2023). Then, the BPHs were removed and stem samples were rapidly collected within the feeding region. The fresh weight of each sample containing four rice stems was not less than 2 grams, which were flash-frozen in liquid nitrogen and stored at -80 in a freezer. Un-infested rice leaf sheaths were collected as control, each treatment included two biological replicates. The rice samples infested by BPHs were named NI-Nip_1 and NI-Nip_2, while the control group was named Nip_1 and Nip_2.

2.4 Total mRNA isolation and Dot-blot hybridization

The Ambion(r) Poly(A) Purist MAG kit (Invitrogen, USA) was taken for total mRNA isolation according to the manufacturer’s instructions. Dot blotting was performed as described previously (Zhang et al., 2021a). The aliquots (10 μ L) of each RNA sample was spotted on a Hybond-N⁺ membrane (Amersham, USA), and cross-linked by UV (1200 \times 100 μ J/cm²). Hybridization was performed for 1 h at 4 °C with anti-m⁶A antibody (#ab208577; Abcam) in 1 \times PBST buffer. The membrane was incubated with alkaline phosphatase-conjugated anti-mouse antibody (#ab98712; Abcam), the specific bands were visualised by adding nitro blue tetrazolium/5-bromo-4-chloro-3-indolyl phosphate as the substrates (Sangon Biotech, China).

2.5 RNA preparation and construction of nanopore sequencing library

Total RNA was isolated using the FastPure Universal Plant Total RNA Isolation Kit (Vazyme, Nanjing, China) according to the manufacturer’s instructions. RNA was cleaned and concentrated by NEB Next Poly(A) mRNA Magnetic Isolation Module (E7490S) according to the manufacturer’s instructions. Each nanopore DRS and transcriptome sequencing sample contained 20 μ g total RNA. Prepared RNA of each sample was used for a nanopore DRS library preparation using the Oxford Nanopore DRS protocol (SQK-RNA002, Oxford Nanopore Technologies) (Yahara et al., 2021). This work was done in collaboration with Wuhan Benagen Technology Co, Ltd, China.

2.6 Preprocessing, alignments, and analysis of novel genes and transcripts

NanoFilt (version: 2.8.0) (De Coster & Rademakers, 2023) was used to filter the raw fastq data and obtain valid data for subsequent analysis (quality score > 7 and sequences longer than 50 bp). Data statistics were performed using SeqKit (version: 0.12.0) (Shen et al., 2016b). Alignment results were then analyzed and quantified using samtools (version: 1.11; parameters: flagstat) (Li et al., 2009). Flair (version: 1.5.0; parameters: -t 20) (Tang et al., 2020) was employed to obtain consistent sequences from the alignment results, then further aligned to the reference genome. Gffcompare software (version: 0.12.1; parameters: -R-C-K-M) (Pertea & Pertea, 2020) were used to compare the transcripts with the known transcripts of the genome and find new transcripts and new genes (FA download link: ftp://ftp.ensemblgenomes.org/pub/plants/release-52/fasta/oryza_sativa/dna/; GTF download link: ftp://ftp.ensemblgenomes.org/pub/plants/release-52/gff3/oryza_sativa/).

2.7 Sequencing data analysis

Raw sequencing data were processed to remove adaptors and low-quality bases, and high-quality reads were aligned with the rice reference genome. The sequenced read coverage at 3'-UTR, coding sequence (CDS), and 5'-UTR of the target transcripts in each library were calculated and normalized. TPM (Transcripts Per Kilobase Million) was used as a measure of transcript expression levels. In the TPM calculation process,

the reads count value for each transcript was divided by its transcript length (in kilobases) to obtain the reads per kilobase coverage (RPK) of the transcript. The RPK values for all transcripts are summed and divided by 1,000,000 to obtain a million-scaling factor. Subsequently, the RPK values are divided by the million-scaling factor to obtain the TPM values. The sum of all TPM values in each sample remains constant, allowing for easier comparison of the proportion of reads mapped to transcripts in each sample. The expression quantification of transcripts was performed using salmon (version: 1.4.0) (Patro et al., 2017), and then subjected to differential expression analysis. DESeq2 (version: 1.26.0) was used as the software for differential expression analysis, with a threshold of padj (p -value) < 0.05 and $|\log_2\text{FoldChange}| > 1$. MINES pipeline (<https://github.com/YeoLab/MINES>) (Lorenz et al., 2020) was used to identify m⁶A modification sites in RNA sequences. Meme (version: 5.3.3) (Bailey et al., 2009) was used to extend two bases up- and down-stream of the m⁶A methylation sites, resulting in a motif comprising five bases. Methylkit (Akalin et al., 2012) was used for differential methylation loci analysis. Gene Ontology (GO) and Kyoto Encyclopedia of Genes and Genomes (KEGG) pathway enrichment analyses of the differentially expressed genes were performed using the Goseq R package and KOBAS 3.0 software, respectively (Ashburner et al., 2000). The enrichment analysis was performed based on the hypergeometric test (Kanehisa et al., 2008).

2.8 Quantitative PCR

Total RNA was isolated as described above. 1 μg of total RNA was reverse-transcribed using the HiScript Reverse Transcriptase (Vazyme, Nanjing, China). Quantitative PCR was performed using Hieff UNICON® Universal Blue qPCR SYBR Green Master Mix (YEASEN, Shanghai, China) (Laveroni & Parks, 2023) according to the manufacturer’s protocol and run in a LightCycler 480 II Real-Time System R (Roche Diagnostics, Basel, Switzerland). We calculated transcript levels of treatment group relative to the control group using the $2^{-\Delta\Delta\tau}$ method (Livak & Schmittgen, 2001) with normalization based on the reference gene *OsEF1-alpha* (Bevitori et al., 2014). The qPCR was repeated three times, with two samples per replicate, and the qPCR primers are listed in Table S23.

2.9 Phytohormones, cellulose, and hemicellulose quantification

DRS-sequenced samples were collected for JA, JA-IIE, and SA content measurement. The fresh weight tissue samples were ground to powder in liquid nitrogen, extracted using ethyl acetate spiked with labeled internal standards (²D6-JA, ²D6-JA-IIE, and ²D4-SA), and analyzed by liquid chromatography-tandem mass spectrometry (HPLC-MS) for phytohormones quantification as previously described (Ji et al., 2021).

For cellulose and hemicellulose quantification, twenty BPH female adults were placed on each rice leaf sheath and continuous feeding for 24 hours. Then, the BPHs were removed and rapid stem sample collection within the feeding region was conducted. The methods of extraction and measurement of cellulose and hemicellulose fractions were previously described (Guo et al., 2018).

2.10 Statistical analysis

Differences among treatments were analyzed with one-way ANOVA followed by Duncan’s multiple range test to compare treatments (or a Student’s *t*-test when only two treatments were compared). We established the filtering criteria correlation between differentially expressed transcripts and differentially directed m⁶A methylation in Ni-Nip vs. Nip group as satisfying both differentially expressed transcripts p -value < 0.05 (based on either RT-qPCR or transcriptome), and a significant m⁶A methylation direction p -value < 0.05 and $|\text{meth diff}| > 10$.

3 RESULTS

3.1 Pre-infestation of rice by BPH female adults reduced subsequent BPH attack

We performed choice and no-choice tests to investigate whether pre-infestation of rice plants by BPH gravid female adults influenced subsequent BPH infestations. In the choice test, BPH nymphs and female adults preferred un-infested rice plants to pre-infested ones (Figure 1a, b). In the no-choice test, the survival rate of nymphs was relatively lower on pre-infested rice than on un-infested rice (Figure 1c). The amount of

honeydew excreted by BPH in pre-infested rice was significantly lower than that in control rice (Figure 1d). Pre-infestation by BPH gravid females therefore increased rice resistance to BPH.

3.2 Widespread m⁶A methylation of rice genomic mRNA with BPH infestation

The genomic mRNA m⁶A methylation modifications and genes expression of un-infested (Nip) and BPH-infested Nip rice (NI-Nip) samples were compared using Nanopore Direct RNA Sequencing (DRS) and Next Generation RNA Sequencing (NGS) respectively (Supporting Information: Figure S1). Reads distribution analysis showed that all samples exhibited considerable m⁶A methylation enrichment within CDS and 3'-UTR regions (Supporting Information: Figure S3). At the genomic level, these unique m⁶A-methylated positions for each treatment were unevenly distributed across each rice chromosome (Figure 1e, Supporting Information: Table S1). Circo plots of the m⁶A methylome in rice genomic RNAs showed that m⁶A distribution density was highly consistent with the corresponding gene density on the same chromosome position in the un-infested sample (Figure 1e).

3.3 BPH infestation decreased rice m⁶A methylation positions

The average number of m⁶A sites in NI-Nip group (79,925) was lower than that in Nip control group (83,011) (Figure 1f, Supporting Information: Table S2), and the dot-blot analysis of m⁶A levels in rice total mRNAs had negative correlation with BPH infestation, implying that m⁶A modification of rice genomic mRNA was repressed under BPH infestation (Figure 1g, Supporting Information: Figure S4). In addition, 42,062 specific m⁶A methylation positions were identified in NI-Nip group, suggesting that 51.3% of positions appeared following BPH infestation (Supporting Information: Figure S5, Table S3). To examine whether there are conserved motifs in m⁶A genes, we compiled transcripts of all m⁶A genes from the four treatments (Supporting Information: Table S4). Four supreme conserved m⁶A modifications motifs were identified: GGACA (36.17%, 35.87%), GGACU (24.12%, 23.70%), GGACC (20.99%, 21.11%), and AGACU (18.72%, 19.32%), respectively, in Nip and NI-Nip groups (Supporting Information: Figure S6). We defined the Nip and NI-Nip consensus m⁶A methylation site as “RGACH” (R=A/G; H=A/U/C), which corresponds with the previously reported in rice and other plants (Parker et al., 2020).

3.4 m⁶A methylation was closely associated with actively expressed genes in BPH-infested plants

We analyzed the Euclidian distance coefficients among gene transcript profiles based on nanopore DRS. The distance coefficients between the replicates were lower than those of other objects, and the tile colors of the two were relatively close (Supporting Information: Figure S7), suggesting their reproducible patterns. These sequenced genes were divided into three groups: transcripts per kilobase of exon model per million mapped reads (TPM) < 1, 1 < TPM < 5, and TPM > 5 (Supporting Information: Table S5). The proportion of gene numbers in each category was calculated and shown as a heatmap (Supporting Information: Figure S8). Rice genes that could be annotated by m⁶A positions were referred to ‘m⁶A genes’ and those that could not be annotated were marked as ‘non-m⁶A genes’ for subsequent analyses. In the Nip and NI-Nip groups, most m⁶A genes were distributed in the highly expressed gene category (TPM > 5). In contrast, non-m⁶A genes were evenly distributed across the three groups and were biased towards gene categories with low expression (TPM < 1). Compared to that in Nip, the proportion of non-m⁶A genes in low expression category was lower in NI-Nip group (Figure 2a, Supporting Information: Figure S8). When the m⁶A and non-m⁶A genes were divided by gene expression categories—high (TPM [?] 1) or low (TPM < 1)—the number of transcripts showing high/low expression was recorded for control Nip and NI-Nip samples (Figure 2b). We found that most genes were m⁶A methylated and distributed in the high expression category in Nip and NI-Nip groups; these gene numbers were enriched upon BPH infestation (Figure 2b). In both Nip and NI-Nip groups, m⁶A-methylated genes were expressed at a higher level than non-m⁶A-methylated genes (Figure 2c). Thus, m⁶A methylation mainly occurred in highly expressed genes in the control and BPH-infested samples, while the m⁶A modified gene numbers increased in the high expression category with BPH infestation.

3.5 m⁶A methylation positively correlated with the transcript expression in BPH-infested rice

We found 21,718 (76.59%) transcripts that showed no significant difference (no change), 3,506 (12.36%) were upregulated and 3,131 (11.04%) were downregulated in BPH-infested plants compared with those in the control plants (Figure 2d, Supporting Information: Figure S9a, Table S6) . A total of 116,817 methylated positions were detected among all expressed transcripts. Among the m⁶A modifications, 63.99%, 17.43%, and 18.58% exhibited no change, or fell into the up- or down-m⁶A directions, respectively (Supporting Information: Table S6). A large proportion of m⁶A modification positions were found in CDS and 3'-UTR, with most showing no change in expression (Figure 2e, Supporting Information: Table S6). Among up-directed m⁶A-methylated transcripts, the number of upregulated transcripts was higher than that of downregulated transcripts (2,094 vs. 856) in the NI-Nip vs. Nip comparison; conversely, in down-directed transcripts, the number of downregulated ones was higher than that of upregulated ones (1,995 vs. 743) (Figure 2e). The correlational heat map showed a strong positive correlation between the m⁶A methylation direction and the corresponding transcript change, with many transcripts and m⁶A modifications exhibiting simultaneous up- or downregulation/direction (Supporting Information: Figure S9b). The abundance of upregulated transcripts that underwent 5'-UTR methylation was higher than that of the downregulated transcripts. However, this tendency was not evident among 3'-UTR methylated transcripts (Figure 2f). Taken together, the m⁶A-methylation differential types in BPH-infested samples were positively correlated with the corresponding transcript regulation types, with transcripts containing different m⁶A methylated functional elements likely involved in diverse transcript regulation.

3.6 BPH infestation regulated m⁶A-methylated genes in rice

The number of transcripts decreased with increasing number of m⁶A modification sites, and most differentially expressed transcripts containing m⁶A modifications had single digit m⁶A sites (Supporting Information: Figure S10). A total of 4.19%, 77.36%, and 18.45% of the m⁶A sites were located on the 5'-UTR, CDS, and 3'-UTR of the differential expressed transcripts in NI-Nip vs. Nip comparison, respectively. Compared with the distribution regions of m⁶A sites in each treatment group, the distribution of these sites tended to be enriched from the 3'-UTR to CDS regions (Figure 2g).

Differential m⁶A-methylated transcripts were subjected to Gene Ontology (GO) (Supporting Information: Figure S11a) and Kyoto Encyclopedia of Genes and Genomes (KEGG) analyses (Supporting Information: Figure S11b). Methylated genes were involved in multiple molecular functions, particularly in structural constituents of ribosomes, translation, and ATP hydrolysis (Supporting Information: Figure S11a, Table S7). The top 25 enriched pathways in KEGG analyses were divided into two categories: genetic information processing and metabolism (Supporting Information: Figure S11b, Table S8). Thus, m⁶A modification is closely related to intracellular metabolism, amino acid metabolism, and secondary metabolite synthesis/metabolism/degradation upon BPH infestation.

3.7 BPH infestation regulated the expression of the main m⁶A modification machinery components

We compared the relative gene expression levels of 5 “WRITER” genes, that is, *OsMTA1* , *OsMTA2* , *OsMTA3* , *OsMTA4* , and *OsFIP* ; 5 “ERASER” genes, namely, *ALKBH9B-1* , *ALKBH9B-2* , *ALKBH10B* , *ALKBH10B-L1* , and *ALKBH10B-L2* ; 12 “READER” genes, that is, *OsYTH01–OsYTH12* ; and 5 “DONOR” genes, namely, *OsSAM1* , *OsSAM1-Like* , *OsSAM2* , *OsSAM2-Like* , and *OsSAM3* in Nip and NI-Nip groups. Based on RT-qPCR analyses, among the five “WRITER” genes, the expression of *OsMTA1* was upregulated while the *OsFIP* gene was suppressed in BPH-infested samples (Figure 3a). For the “ERASER” genes, the expression of *ALKBH9B-1* was slightly increased in the BPH-infested samples, whereas those of *ALKBH9B-2* and *ALKBH10B* were downregulated (Figure 3b). In the “READER” genes, the *OsYTH02* , *OsYTH04* , *OsYTH07* , *OsYTH08* , *OsYTH11* , and *OsYTH12* expression levels were significantly upregulated in BPH-infested samples. Meanwhile, the expression of the *OsYTH01* , *OsYTH05* , *OsYTH09* , and *OsYTH10* genes was significantly suppressed (Figure 3c). Compared to those in control Nip, the expression levels of all five methyl “DONOR” synthesis genes were upregulated in NI-Nip (Figure 3d). The results of the transcriptome analyses and RT-qPCR were basically consistent, highlighting the reliability of the transcriptome sequencing data (Figure 3).

The dynamic changes in m⁶A positions in the m⁶A methylation machinery components were tested. Given that most genes were modified by different m⁶A sites, we counted the numbers of m⁶A methylation sites for each gene and further categorized them into three direction types, that is, up-direction (Up), down-direction (Down), and no significant difference (No change) between the NI-Nip and Nip groups (Supporting Information: Table S9). Among the “DONOR” genes, only *OsSAM2* exhibited an up-m⁶A site. For the “WRITER” genes, *OsMTA1–OsMTA4* genes contained the up-directed m⁶A site, while *OsFIP* showed a down-trend of m⁶A sites. For the “ERASER” genes, *ALKBH9B-1* and *ALKBH10B* contained the up-directed m⁶A sites, while *ALKBH9B-2* showed a down-trend in m⁶A sites. Regarding the “READER” genes, *OsYTH07*, *OsYTH08*, and *OsYTH11* only contained up-directed differential m⁶A sites, while *OsYTH01*, *OsYTH06*, *OsYTH09*, and *OsYTH10* only showed down-directed differential m⁶A sites. The *OsYTH02*, *OsYTH03*, *OsYTH05*, and *OsYTH12* genes contained more than 10 differential patterns of m⁶A positions in the NI-Nip vs. Nip comparison, including up-, down-, and non-directed m⁶A sites (Supporting Information: Table S9, S10).

A filtering criteria was established to determine a correlation between the transcription and m⁶A methylation level of the target genes in the NI-Nip vs. Nip comparison group as a transcriptional expression fold change < 0.5 or > 2, along with a significant m⁶A methylation trend $p < 0.05$, and $|\text{meth diff}| > 10$ (Supporting Information: Table S6, S10). Genes like *OsMTA1* was upregulated and showed accompanying upregulated m⁶A methylation, that is, the number of upregulated m⁶A sites was higher than that of downregulated m⁶A sites in this transcript. Genes such as *OsFIP* was downregulated and exhibited downregulated m⁶A methylation, that is, the number of downregulated m⁶A sites was higher than that of the upregulated m⁶A sites (Figure 3; Supporting Information: Table S9, S10). We identified the *OsSAM2* gene in the “DONOR” category, *OsMTA1* and *OsFIP* genes in “WRITER” category, *ALKBH9B-2* gene in the “ERASER” category, and *OsYTH01*, *OsYTH05*, *OsYTH07–OsYTH12* genes in the “READER” category. These genes not only differentially expressed but also included the differential m⁶A methylation sites with the same regulatory trend (Figure 3e). This indicated that m⁶A modification may positively regulate the transcription of target transcripts. m⁶A modifications were observed in genes responsible for plant m⁶A methylation machinery, highlighting their potential role in regulating target gene expression dynamics. This mechanism may be an important post-translational regulatory strategy in rice, particularly in response to BPH infestation.

3.8 BPH infestation regulated m⁶A modifications and expression of BPH resistance genes

The expression levels of nine *Bphs* were analyzed by RT-qPCR, and combined with a detailed analysis of the m⁶A modification positions. In the BPH-infected group, the expression of 8 candidate genes, except *Bph6*, were upregulated. Fold changes in *Bph14*, *Bph30*, *Bph40*, and *Bphi008a* were 7.80, 2.01, 1.59, and 7.57, respectively (Figure 4a). Four genes showed upregulated m⁶A modifications: *Bph14* contained 12 upregulated and 1 downregulated differential m⁶A site, *Bph30* and *Bph40* contained relatively more upregulated differential m⁶A sites, whereas *Bph6* only contained 5 downregulated differential m⁶A sites (Supporting Information: Table S11, S12). All the genes showed a positive correlation between the direction of m⁶A modification and transcript regulation, highlighting that m⁶A modification is involved in the regulation of rice *Bph* genes expression.

3.9 BPH infestation altered the expression and m⁶A modification of cellulose synthesis-related genes

Both *Bph30* and *Bph40* genes were significantly upregulated upon BPH infestation (Figure 4a). Therefore, the potential correlation between m⁶A levels and the expression of rice genes involved in cellulose and hemicellulose synthesis was analyzed. Among thirteen candidate cellulose synthesis genes which containing m⁶A modification sites, eight genes were upregulated in BPH-infested plants (Figure 4b). Moreover, there were total 39 up- and 23 down-directed differential m⁶A modification positions among the 13 cellulose synthesis genes, 5 of which showed up-trending m⁶A methylation, that is, the number of up-directed m⁶A sites was higher than that of down-directed m⁶A sites (Supporting Information: Table S11, S13). m⁶A modifications and the relative expression of genes in cellulose synthesis were positively correlated, suggesting that m⁶A modification is largely involved in the synthesis of cellulose. Additionally, four of the six hemicellulose

synthesis (*CSLF4* , *CSLHL* , *IRX10* , and *IRX14*) were upregulated, while *IRX9* was downregulated in BPH-infested plants (Figure 4c). However, only four genes (*CSLF2* , *CSLHL* , *IRX9* , and *IRX14*) were detected with m⁶A positions (Supporting Information: Table S11, S14) and no fixed regular patterns were found.

Moreover, the contents of cellulose and hemicellulose were measured. BPH infestation induced cellulose and hemicellulose accumulation in rice. This degree of induction was more pronounced for cellulose accumulation than for hemicellulose (Figure 4d,e), which were validated the RT-qPCR and transcriptome data. Taken together, BPH infestation activated the expression and m⁶A modification of cellulose but not apparent in hemicellulose synthesis-related genes, and was more prominent in cellulose synthesis.

3.10 BPH infestation activated defense-related phytohormones pathways though dynamic m⁶A modifications

We investigated whether anti-herbivore defense hormones JA and SA metabolic pathways are regulated by m⁶A modification and whether the expression profiles of their metabolic genes are altered by BPH infestation in rice. All 9 selected biosynthesis genes in the JA pathway, except downregulated *OsLOX5* , were upregulated in BPH-infested plants (Figure 5a). Expression levels of all the JA-responsive genes, *OsPR5-1* , *OsPR10* , and *OsRbohC-F* , were downregulated in BPH-infested samples; the remaining genes, apart from non-regulated *OsWRKY10* , were significantly upregulated (Figure 5b,c). Among the JA biosynthesis genes, *OsAOS2* , *OsJMT1* , and *OsLOX8* only exhibited upregulated differential m⁶A sites; *OsAOS1* , *OsLOX2* , and *OsLOX5* exhibited both up-, and down-directed m⁶A sites (Supporting Information: Table S15, S16). For JA-responsive genes, *OsPR2* , *OsPR5-2* , *OsPR5-3* , *OsPR5-4* , *OsMYB2* , and *OsWRKY28* only contained up-directed differential m⁶A sites, while *OsPR5-1* , *OsPR10* , *OsRbohD* , and *OsRbohF* only showed down-directed differential m⁶A sites. *OsRbohB* , *OsRbohC* , and *OsRbohE* contained both up- and down-directed m⁶A sites (Supporting Information: Table S15, S17). Most upregulated genes showed a positive correlation with the up-directed m⁶A modification positions, such as *OsJMT1* , *OsAOS1* , *OsAOS2* , and *OsLOX8* in biosynthesis genes, and *OsPR2* , *OsPR5-2* , *OsPR5-3* , *OsPR5-4* , *OsMYB2* , and *OsWRKY28* in responsive genes. Both m⁶A modification and the relative expression of *OsPR5-1* , *OsPR10* , *OsLOX5* , and *OsRbohC-F* were significantly downregulated in BPH-infested plants (Figure 5a-c; Supporting Information: Table S15-17).

In the SA pathway, all candidate biosynthesis-related genes were upregulated in BPH-infested samples (Figure S12a). Among the response-related genes, *OsPR1-12* , *OsPR1-51* , *OsPR1a* , *OsPR1b* , and *OsWRKY45* were upregulated, while *OsPR1-21* , and *OsPR1-101* were downregulated in BPH-infested samples (Figure S12b). Regarding the m⁶A position direction, *OsCM* and *OsWRKY45* only exhibited up-directed differential m⁶A sites; *OsICS1* and *OsPR1-101* contained down-directed differential m⁶A sites; and *OsEDS1* , *OsPAL* , and *OsPAL1* showed both up- and down-directed m⁶A sites (Supporting Information: Table S15, S18, S19). The m⁶A modification level of SA pathway-related genes also showed a positive correlation with transcriptional regulation. The genes that followed such pattern included *OsPAL1* and *OsCM* in the biosynthesis genes and *OsPR1-101* and *OsWRKY45* in the responsive genes (Supporting Information: Figure S12; Table S15, S18, S19). However, the proportion of m⁶A modified genes was lower than that of the JA pathway-related genes.

BPH infestation successfully induced phytohormones accumulation in plants. This degree of induction was more pronounced for JA production than for SA (Figure 5d,e; Supporting Information: Figure S12c), which validated the RT-qPCR and transcriptome data of the related transcripts. These were accompanied by dynamic m⁶A methylation modification and gene expression changes in major hormonal pathway-related genes, especially in genes related to the JA metabolic pathway.

3.11 BPH infestation affected m⁶A modification of genes involved in growth-related phytohormones pathways

The overall m⁶A methylation position in rice was significantly attenuated by the BPH treatment (Figure 1f,g; Supporting Information: S4). However, the defense-related pathways were activated by BPH infestation

which was accompanied by a large proportion of upregulated transcripts and m⁶A methylation sites (Figure 4, 5; Table S11, S15). Plant defense against herbivores is costly and is often associated with growth repression (Deng et al., 2020). We then explored m⁶A modification and transcriptional regulation of genes involved in plant growth-related phytohormones pathways especially auxin and gibberellin (GA).

Among the selected 32 genes containing m⁶A modification sites, 11 up- and 79 down-directed m⁶A modification positions were present in BPH-infested plants compared with those in the un-infested plants. A total of 27 genes were found to have down-directed m⁶A sites, among which 26 genes showed down-trending m⁶A methylation; that is, the number of down-directed m⁶A sites was higher than up-directed m⁶A sites (Supporting Information: Table S20). For transcriptome regulation, 27 of these 32 transcripts were significantly downregulated in BPH-infested plants, 25 of which displayed down-trending m⁶A methylation (Figure 6a-d, Supporting Information: Table S20-S22). This indicated a positive correlation between m⁶A modifications and the expression of key genes responsible for rice growth. In contrast, for the GA metabolic process, three of the five candidate genes were upregulated in the BPH-infested group. There were 9 up- and 5 down-directed m⁶A modification positions in the BPH-infested plants compared to those in the un-infested plants. m⁶A modifications and gene expression were also positively correlated (Figure 6e, Supporting Information: Table S20, S22). The m⁶A modification levels of auxin pathway- and GA biosynthesis-related genes were significantly attenuated under BPH attack. This was accompanied by the downregulated expression of these transcripts. Meanwhile, m⁶A modification was involved in the activation of GA catabolism-related genes. Thus, rice growth was restricted during BPH attack to optimize resource allocation for plant defense though affecting m⁶A modification of genes involved in defense- and growth-related phytohormones pathways.

4 DISCUSSION

A promising new area of RNA epigenetic research has emerged following the identification of m⁶A modifications in numerous organisms. We are only beginning to understand the m⁶A modification's involvement in this processes (Shinde et al., 2023). In this study, we focused on the most important and destructive pest influencing rice production, that is, BPH, to investigate the effect of BPH infestation on rice m⁶A methylation and the relationship between m⁶A and the expression of target gene bodies involved in plant defense and growth, thereby revealing its overall regulatory patterns (Figure 7). To the best of our knowledge, no studies has been previously reported in plants coping with herbivore stress.

4.1 Genome-wide m⁶A distributions in rice

The distribution map of m⁶A modifications throughout the mammalian genome has been extensively assessed (Gokhale et al., 2016). Among plants, there are more reports on m⁶A modification sites in *Arabidopsis* genomic mRNA (Parker et al., 2021), and the number of reports on rice is gradually increasing (Wang et al., 2023a). We identified about 80,000 m⁶A modification sites in un-infested and BPH-infested Nip rice using the nanopore DRS, a powerful approach that can detect single methylation modification sites on mRNA (Supporting Information: Figure S4). Which was similar to 81,722 m⁶A sites previously reported in the Nipponbare rice cultivar (Yu et al., 2023). Most gene density was consistent with the density of the m⁶A methylome, and m⁶A modifications were primarily distributed on rice chromosomes 1, 2, and 3 (Figure 1e). A marked distribution pattern of m⁶A modifications was observed on chromosomes 1, 2, 3, 5, 6, 7, 8, and 12, which appeared as a dense and sparse distribution with higher density at both ends and lower density in the middle. Conversely, on chromosomes 4, 10, and 11, the m⁶A modification exhibited a distribution with a higher density on one side and a lower density on the other. These distributions may be related to the organization and arrangement of genes on the chromosomes (Figure 1e). m⁶A modification predominantly occurs on exons and splicing sites of RNA precursors, suggesting a certain level of selectivity in m⁶A modification (He et al., 2023). However, genes on different chromosomes exhibit variations in the lengths and quantities of exons and introns. Our results showed that m⁶A modification was most densely distributed in the CDS region, followed by that in the 3'-UTR, and least in the 5'-UTR (Supporting Information: Figure S3). This distribution pattern is conserved in several important crops, including rice (Zhang et al., 2021a), maize (*Zea mays*) (Miao et al., 2020), wheat (*T. aestivum*) (Zhang et al., 2021b), and tomato (*Solanum lycopersicum*) (Hu et al., 2022). In mature strawberry fruit (Zhou et al., 2021), as well as in apple (Guo et

al., 2022) and cabbage leaves (Liu et al., 2020a). Thus, m⁶A modification mainly in the CDS region may be developmental or tissue specific. The factors underlying this distribution pattern and the detailed biological functions of m⁶A modifications in plants remain largely unknown; these aspects require further investigation.

4.2 m⁶A methylation regulated the expression of genes

m⁶A primarily occurs in highly expressed genes during BPH infestation (Figure 2a,b). In contrast, m⁶A mainly occurs in rice genes with low expression levels during viral infection (Zhang et al., 2021a). Responsive m⁶A modification is sensitive and complex during biological stress, and different stressors may induce m⁶A methylation in genes with varying expression levels. Through KEGG analyses, we identified differentially expressed transcripts in many pathways containing m⁶A modifications (Supporting Information: Figure S11). Four component genes in the principal constituents of rice m⁶A modification machinery can undergo m⁶A modification. Their relative expression levels showed considerable variations (Figure 3a–d). Thus, m⁶A machinery can govern the expression of key component genes via m⁶A methylation, resulting in significant alterations in overall cellular m⁶A levels in rice when confronted with BPH infestation. This suggests a potential role for m⁶A in modulating plant defense against insects.

We found differential regulatory patterns of m⁶A modifications in gene expression across different plant specific BPH response pathways. The m⁶A modification direction of genes related to the four methylation components, and major phytohormone pathways (which including JA, SA, auxin, GA), *Bph*, and cellulose synthesis, showed a positive correlation with the target transcript expression (Figure 3-6; Supporting Information: Table S9, S11, S15, S20). No apparent regulatory patterns were found for the hemicellulose synthesis-related genes (Figure 4C; Supporting Information: Table S14). Thus, the levels of m⁶A modification display specific enrichment patterns depends on the type of metabolic pathways. Based on studies on regulation of m⁶A modifications in rice by various viruses and fungi (Shi et al., 2019; Zhang et al., 2021a), our findings suggest a potential role for m⁶A in modulating plant defense against insects.

4.3 m⁶A methylation regulated plant defense and growth upon insect infestation

Growth reduction is commonly associated with herbivore attack and defense activation, which is known as the growth-defense trade-off (He et al., 2022). Therefore, plants decide when to grow or defend themselves to optimize their fitness in a changing environment. Research into the molecular mechanisms underlying these growth-defense trade-offs has shown that phytohormones signaling and crosstalk between phytohormones play central roles (Huot et al., 2014; He et al., 2022). Auxin, GA and JA are important growth-and defense-related phytohormones, respectively (Yang et al., 2012). As one of the earliest phytohormones identified, auxin plays an essential role in most aspects of plant growth and development, and also play a vital role in plant defense against diverse pathogens (Spaepen & Vanderleyden, 2011). In *Arabidopsis*, the core JA-responsive basic helix-loop-helix transcription factor MYC2-mediated repression expression of the growth regulator PLT integrates JA action into the auxin pathway in regulating root meristem activity and stem cell niche maintenance (Chen et al., 2011). BPH attack activates GA catabolism in rice plants via two GA catabolism genes, that is, *GA2ox3* and *GA2ox7*, contribute to BPH-induced growth restriction and are upregulated by JA signaling. The JA-responsive transcription factor MYC2 binds to the promoters of *GA2ox3* and *GA2ox7* to regulate their expression. Therefore, the MYC2-GA2ox module regulates the growth-defense trade-off when BPH attacks rice, which provides a mechanism for phytohormone crosstalk (Jin et al., 2023).

Although the overall m⁶A methylation of rice was constrained by BPH damage (Figure 1f,g), JA signaling pathway-related genes were altered and accompanied by a predominance of upregulated transcripts and up-directed m⁶A methylation sites (Figure 5, Supporting Information: Table S15). Some key genes responsible for rice growth pathways have shown distinct m⁶A-modification directions from JA pathway. This was reflected in attenuated m⁶A-modification levels of auxin and GA biosynthesis-related genes under BPH attack, which contributed to the downregulated expression of these transcripts. The rice GA catabolism process was activated after BPH infection, and the significantly upregulated *OsGA2ox3*, *OsWRKY71*, and *OsCRY1b* genes displayed a positive correlation between m⁶A modifications and gene expression (Figure

6, Supporting Information: Table S20-S22). This indicated that plant defense was activated but growth was suppressed during BPH attack, this growth–defense trade-off was likely regulated by m⁶A methylation-mediated Auxin, GA, and JA pathways in BPH-infested rice.

Overall, m⁶A modification levels were repressed under BPH infestation, with m⁶A primarily modifying highly expressed genes. Here, we proposed a simplified model for rice m⁶A RNA methylation modulation in key defense and growth pathways induced by BPH infestation (Figure 7). m⁶A modification was positively correlated with the expression of key genes, mainly in insect–stress response and growth pathways in rice, and may have contributed to plants prioritizing defense overgrowth during BPH attack.

ACKNOWLEDGEMENTS

The authors are grateful to Jing Li, Liangxuan Qi and Yaxuan Chen for their help with the experiments and data analysis. We would like to thank Editage (www.editage.cn) for English language editing.

CONFLICT OF INTEREST STATEMENT

The authors declare no competing interests.

AUTHOR CONTRIBUTIONS

Shuai Li, Xinyang Tan, Zhen He and Rui Ji conceived the project, performed the experiments, analyzed the data, and wrote the manuscript. Rui Ji, Jichao Fang, Ary A. Hoffmann, and Chunqing Zhao supervised the project and edited the English language. Yali Li, Liu Yang and Lei Jiang helped in the sequencing data handling and arrangement. All authors read and approved the final manuscript.

REFERENCES

- Akalin, A., Kormaksson, M., Li, S., Garrett-Bakelman, F.E., Figueroa, M.E., Melnick, A., Mason, C.E. (2012). methylKit: a comprehensive R package for the analysis of genome-wide DNA methylation profiles. *Genome Biol.* 13: R87.
- Ashburner, M., Ball, C.A., Blake, J.A., Botstein, D., Butler, H., Cherry, J.M., Davis, A.P., Dolinski, K., Dwight, S.S., Eppig, J.T., Harris, M.A., Hill, D.P., Issel-Tarver, L., Kasarskis, A., Lewis, S., Matese, J.C., Richardson, J.E., Ringwald, M., Rubin, G.M., Sherlock, G. (2000). Gene ontology: tool for the unification of biology. The gene ontology consortium. *Nat Genet.* 25: 25-29.
- Bailey, T.L., Boden, M., Buske, F.A., Frith, M., Grant, C.E., Clementi, L., Ren, J., Li, W.W., Noble, W.S. (2009). MEME SUITE: tools for motif discovery and searching. *Nucleic Acids Res.* 37: W202-208.
- Bass, C., Carvalho, R.A., Oliphant, L., Puinean, A.M., Field, L.M., Nauen, R., Williamson, M.S., Moores, G., Gorman, K. (2011). Overexpression of a cytochrome P450 monooxygenase, CYP6ER1, is associated with resistance to imidacloprid in the brown planthopper, *Nilaparvata lugens*. *Insect Mol Biol.* 20: 763-773.
- Berthelie, J., Furci, L., Asai, S., Sadykova, M., Shimazaki, T., Shirasu, K., Saze, H. (2023). Long-read direct RNA sequencing reveals epigenetic regulation of chimeric gene-transposon transcripts in *Arabidopsis thaliana*. *Nat Commun.* 14: 3248.
- Bevitori, R., Oliveira, M.B., Grossi-de-Sá, M.F., Lanna, A.C., da Silveira, R.D., Petrofeza, S. (2014). Selection of optimized candidate reference genes for RT-qPCR normalization in rice (*Oryza sativa*L.) during *Magnaporthe oryzae* infection and drought. *Genet Mol Res.* 13: 9795-9805.
- Bodi, Z., Zhong, S., Mehra, S., Song, J., Graham, N., Li, H., May, S., Fray, R.G. (2012). Adenosine methylation in *Arabidopsis* mRNA is associated with the 3' End and reduced levels cause developmental defects. *Front Plant Sci.* 3: 48.
- Chen, Q., Sun, J., Zhai, Q., Zhou, W., Qi, L., Xu, L., Wang, B., Chen, R., Jiang, H., Qi, J., Li, X., Palme, K., Li, C. (2011). The basic helix-loop-helix transcription factor MYC2 directly represses PLETHORA

expression during jasmonate-mediated modulation of the root stem cell niche in Arabidopsis. *Plant Cell*. 23: 3335-3352.

Chen, Y., Lai, Y., Liu, R., Yao, L., Yu, X.Q., Wang, X. (2023). Transcriptome-wide analysis of mRNA^{m6}-methyladenosine modification in the embryonic development of *Spodoptera frugiperda*. *Insect Sci*.

Dabravolski, S.A., Isayenkov, S.V. (2023). The regulation of plant cell wall organisation under salt stress. *Front Plant Sci*. 14: 1118313.

De Coster, W., Rademakers, R. (2023). NanoPack2: population-scale evaluation of long-read sequencing data. *Bioinformatics*. 39: pii: 7160911.

Deng, Y., Ning, Y., Yang, D.L., Zhai, K., Wang, G.L., He, Z. (2020). Molecular basis of disease resistance and perspectives on breeding strategies for resistance improvement in crops. *Mol Plant*. 13: 1402-1419.

Dominissini, D., Moshitch-Moshkovitz, S., Schwartz, S., Salmon-Divon, M., Ungar, L., Osenberg, S., Cesarikas, K., Jacob-Hirsch, J., Amariglio, N., Kupiec, M., Sorek, R., Rechavi, G. (2012). Topology of the human and mouse m⁶A RNA methylomes revealed by m⁶A-seq. *Nature*. 485: 201-206.

Du, B., Zhang, W., Liu, B., Hu, J., Wei, Z., Shi, Z., He, R., Zhu, L., Chen, R., Han, B., He, G.C. (2009) Identification and characterization of Bph14, a gene conferring resistance to brown planthopper in rice. *Proc Natl Acad Sci U S A*. 106: 22163-8.

Duan, H.C., Wei, L.H., Zhang, C., Wang, Y., Chen, L., Lu, Z., Chen, P.R., He, C., Jia, G. (2017). ALKBH10B is an RNA^{m6}-methyladenosine demethylase affecting Arabidopsis floral transition. *Plant Cell*. 29: 2995-3011.

Erb, M., Reymond, P. (2019). Molecular interactions between plants and insect herbivores. *Annu Rev Plant Biol*. 70: 527-557.

Gao, Y., Liu, X., Jin, Y., Wu, J., Li, S., Li, Y., Chen, B., Zhang, Y., Wei, L., Li, W., Li, R., Lin, C., Reddy, A.S.N., Jaiswal, P., Gu, L. (2022). Drought induces epitranscriptome and proteome changes in stem-differentiating xylem of *Populus trichocarpa*. *Plant Physiol*. 190: 459-479.

Gokhale, N.S., McIntyre, A.B.R., McFadden, M.J., Roder, A.E., Kennedy, E.M., Gandara, J.A., Hopcraft, S.E., Quicke, K.M., Vazquez, C., Willer, J., Ilkayeva, O.R., Law, B.A., Holley, C.L., Garcia-Blanco, M.A., Evans, M.J., Suthar, M.S., Bradrick, S.S., Mason, C.E., Horner, S.M. (2016). RNA^{m6}-methyladenosine in *Flaviviridae* viral RNA genomes regulates infection. *Cell Host Microbe*. 20: 654-665.

Guo, J., Wang, H., Guan, W., Guo, Q., Wang, J., Yang, J., Peng, Y., Shan, J., Gao, M., Shi, S., Shangguan, X., Liu, B., Jing, S., Zhang, J., Xu, C., Huang, J., Rao, W., Zheng, X., Wu, D., Zhou, C., Du, B., Chen, R., Zhu, L., Zhu, Y., Walling, L.L., Zhang, Q., He, G. (2023). A tripartite rheostat controls self-regulated host plant resistance to insects. *Nature*. 618: 799-807.

Guo, J., Xu, C., Wu, D., Zhao, Y., Qiu, Y., Wang, X., Ouyang, Y., Cai, B., Liu, X., Jing, S., Shangguan, X., Wang, H., Ma, Y., Hu, L., Wu, Y., Shi, S., Wang, W., Zhu, L., Xu, X., Chen, R., Feng, Y., Du, B., He, G. (2018). Bph6 encodes an exocyst-localized protein and confers broad resistance to planthoppers in rice. *Nat Genet*. 50: 297-306.

Guo, T., Liu, C., Meng, F., Hu, L., Fu, X., Yang, Z., Wang, N., Jiang, Q., Zhang, X., Ma, F. (2022). The m⁶A reader MhYTP2 regulates MdMLO19 mRNA stability and antioxidant genes translation efficiency conferring powdery mildew resistance in apple. *Plant Biotechnol J*. 20: 511-525.

Hasan, S., Huang, L., Liu, Q., Perlo, V., O'Keeffe, A., Margarido, G.R.A., Furtado, A., Henry, R.J. (2022). The long read transcriptome of rice (*Oryza sativa* ssp. japonica var. Nipponbare) reveals novel transcripts. *Rice (N Y)*. 15: 29.

He, P.C., Wei, J., Dou, X., Harada, B.T., Zhang, Z., Ge, R., Liu, C., Zhang, L.S., Yu, X., Wang, S., Lyu, R., Zou, Z., Chen, M., He, C. (2023). Exon architecture controls mRNA m⁶A suppression and gene expression. *Science*. 379: 677-682.

- He, Z., Webster, S., He, S.Y. (2022). Growth-defense trade-offs in plants. *Curr Biol.* 32: R634-r639.
- Hou, X., Lee, L.Y., Xia, K., Yan, Y., Yu, H. (2010). DELLAs modulate jasmonate signaling via competitive binding to JAZs. *Dev Cell.* 19: 884-894.
- Hu, J., Cai, J., Umme, A., Chen, Y., Xu, T., Kang, H. (2022). Unique features of mRNA m⁶A methylomes during expansion of tomato (*Solanum lycopersicum*) fruits. *Plant Physiol.* 188: 2215-2227.
- Hu, J., Zhou, J., Peng, X., Xu, H., Liu, C., Du, B., Yuan, H., Zhu, L., He, G. (2011). The Bphi008a gene interacts with the ethylene pathway and transcriptionally regulates MAPK genes in the response of rice to brown planthopper feeding. *Plant Physiol.* 156: 856-872.
- Huot, B., Yao, J., Montgomery, B.L., He, S.Y. (2014). Growth-defense tradeoffs in plants: a balancing act to optimize fitness. *Mol Plant.* 7: 1267-1287.
- Ji, R., Fu, J., Shi, Y., Li, J., Jing, M., Wang, L., Yang, S., Tian, T., Wang, L., Ju, J., Guo, H., Liu, B., Dou, D., Hoffmann, A.A., Zhu-Salzman, K., Fang, J. (2021). Vitellogenin from planthopper oral secretion acts as a novel effector to impair plant defenses. *New Phytol.* 232: 802-817.
- Jin, G., Qi, J., Zu, H., Liu, S., Gershenzon, J., Lou, Y., Baldwin, I.T., Li, R. (2023). Jasmonate-mediated gibberellin catabolism constrains growth during herbivore attack in rice. *Plant Cell.* 35: 3828-3844.
- Kanehisa, M., Araki, M., Goto, S., Hattori, M., Hirakawa, M., Itoh, M., Katayama, T., Kawashima, S., Okuda, S., Tokimatsu, T., Yamanishi, Y. (2008). KEGG for linking genomes to life and the environment. *Nucleic Acids Res.* 36: D480-484.
- Laveroni, S.L., Parks, V.R. (2023). Quantitative PCR of alu repeats using PowerUp SYBR(r) Green Master Mix. *Methods Mol Biol.* 2685: 149-174.
- Li, C.P., Wu, D.H., Huang, S.H., Meng, M., Shih, H.T., Lai, M.H., Chen, L.J., Jena, K.K., Hechanova, S.L., Ke, T.J., Chiu, T.Y., Tsai, Z.Y., Chen, G.K., Tsai, K.C., Leu, W.M. (2023). The Bph45 gene confers resistance against brown planthopper in rice by reducing the production of limonene. *Int J Mol Sci.* 24: pii: ijms24021798.
- Li, H., Handsaker, B., Wysoker, A., Fennell, T., Ruan, J., Homer, N., Marth, G., Abecasis, G., Durbin, R. (2009). The sequence Alignment/Map format and SAMtools. *Bioinformatics.* 25: 2078-2079.
- Li, J., Halitschke, R., Li, D., Paetz, C., Su, H., Heiling, S., Xu, S., Baldwin, I.T. (2021a). Controlled hydroxylations of diterpenoids allow for plant chemical defense without autotoxicity. *Science.* 371: 255-260.
- Li, M., Yu, G., Cao, C., Liu, P. (2021b). Metabolism, signaling, and transport of jasmonates. *Plant Commun.* 2: 100231.
- Liu, G., Wang, J., Hou, X. (2020a). Transcriptome-wide N⁶-methyladenosine (m⁶A) methylome profiling of heat stress in Pak-choi (*Brassica rapa* ssp. *chinensis*). *Plants (Basel).* 9: pii: plants9091080.
- Liu, J., Dou, X., Chen, C., Chen, C., Liu, C., Xu, M.M., Zhao, S., Shen, B., Gao, Y., Han, D., He, C. (2020b). N⁶-methyladenosine of chromosome-associated regulatory RNA regulates chromatin state and transcription. *Science.* 367: 580-586.
- Liu, M.Y., Hong, G.J., Li, H.J., Bing, X.L., Chen, Y.M., Jing, X.F., Gershenzon, J., Lou, Y.G., Baldwin, I.T., Li, R. (2023) Sakuranetin protects rice from brown planthopper attack by depleting its beneficial endosymbionts. *Proc Natl Acad Sci U S A.* 120: e2305007120.
- Livak, K.J., Schmittgen, T.D. (2001). Analysis of relative gene expression data using real-time quantitative PCR and the 2(-Delta Delta C(T)) Method. *Methods.* 25: 402-408.
- Lorenz, D.A., Sathe, S., Einstein, J.M., Yeo, G.W. (2020). Direct RNA sequencing enables m⁶A detection in endogenous transcript isoforms at base-specific resolution. *RNA.* 26: 19-28.

- Martinez-Perez, M., Aparicio, F., Lopez-Gresa, M.P., Belles, J.M., Sanchez-Navarro, J.A., Pallas, V. (2017). Arabidopsis m⁶A demethylase activity modulates viral infection of a plant virus and the m⁶A abundance in its genomic RNAs. *Proc Natl Acad Sci U S A*. 114: 10755-10760.
- Miao, Z., Zhang, T., Qi, Y., Song, J., Han, Z., Ma, C. (2020). Evolution of the RNA N⁶-methyladenosine methylome mediated by genomic duplication. *Plant Physiol*. 182: 345-360.
- Muduli, L., Radhan, S.K.P., Mishra, A., Bastia, D.N., Samal, K.C., Agrawal, P.K., Dash, M. (2021). Understanding brown planthopper resistance in rice: genetics, biochemical and molecular breeding approaches. *Rice Science*. 28: 532-546.
- Otuka, A. (2013). Migration of rice planthoppers and their vectored re-emerging and novel rice viruses in east Asia. *Front Microbiol*. 4: 309.
- Pannak, S., Wanchana, S., Aesomnuk, W., Pitaloka, M.K., Jamboonsri, W., Siangliw, M., Meyers, B.C., Toojinda, T., Arikrit, S. (2023). Functional Bph14 from Rathu Heenati promotes resistance to BPH at the early seedling stage of rice (*Oryza sativa* L.) as revealed by QTL-seq. *Theor Appl Genet*. 136: 25.
- Parker, M.T., Knop, K., Sherwood, A.V., Schurch, N.J., Mackinnon, K., Gould, P.D., Hall, A.J., Barton, G.J., Simpson, G.G. (2020). Nanopore direct RNA sequencing maps the complexity of Arabidopsis mRNA processing and m⁶A modification. *Elife*. 9: pii: 49658.
- Parker, M.T., Knop, K., Zacharaki, V., Sherwood, A.V., Tome, D., Yu, X., Martin, P.G., Beynon, J., Michaels, S.D., Barton, G.J., Simpson, G.G. (2021). Widespread premature transcription termination of *Arabidopsis thaliana* NLR genes by the spen protein FPA. *Elife*. 10: pii: 65537.
- Patro, R., Duggal, G., Love, M.I., Irizarry, R.A., Kingsford, C. (2017). Salmon provides fast and bias-aware quantification of transcript expression. *Nat Methods*. 14: 417-419.
- Perteau, G., Perteau, M. (2020). GFF Utilities: GffRead and GffCompare. *F1000Res*. 9.
- Pratanwanich, P.N., Yao, F., Chen, Y., Koh, C.W.Q., Wan, Y.K., Hendra, C., Poon, P., Goh, Y.T., Yap, P.M.L., Chooi, J.Y., Chng, W.J., Ng, S.B., Thiery, A., Goh, W.S.S., Goke, J. (2021). Identification of differential RNA modifications from nanopore direct RNA sequencing with xPore. *Nat Biotechnol*. 39: 1394-1402.
- Reymond, P. (2021). Receptor kinases in plant responses to herbivory. *Curr Opin Biotechnol*. 70: 143-150.
- Sekula, B., Ruszkowski, M., Dauter, Z. (2020). S-adenosylmethionine synthases in plants: Structural characterization of type I and II isoenzymes from *Arabidopsis thaliana* and *Medicago truncatula*. *Int J Biol Macromol*. 151: 554-565.
- Shen, L., Liang, Z., Gu, X., Chen, Y., Teo, Z.W., Hou, X., Cai, W.M., Dedon, P.C., Liu, L., Yu, H. (2016a). N(6)-methyladenosine RNA modification regulates shoot stem cell fate in Arabidopsis. *Dev Cell*. 38: 186-200.
- Shen, W., Le, S., Li, Y., Hu, F. (2016b). SeqKit: A cross-platform and ultrafast toolkit for FASTA/Q file manipulation. *PLoS One*. 11: e0163962.
- Shi, S., Wang, H., Nie, L., Tan, D., Zhou, C., Zhang, Q., Li, Y., Du, B., Guo, J., Huang, J., Wu, D., Zheng, X., Guan, W., Shan, J., Zhu, L., Chen, R., Xue, L., Walling, L.L., He, G. (2021). Bph30 confers resistance to brown planthopper by fortifying sclerenchyma in rice leaf sheaths. *Mol Plant*. 14: 1714-1732.
- Shi, Y., Wang, H., Wang, J., Liu, X., Lin, F., Lu, J. (2019). N⁶-methyladenosine RNA methylation is involved in virulence of the rice blast fungus *Pyricularia oryzae* (syn. *Magnaporthe oryzae*). *FEMS Microbiol Lett*. 366: pii: 5238720.
- Shinde, H., Dudhate, A., Kadam, U.S., Hong, J.C. (2023). RNA methylation in plants: An overview. *Front Plant Sci*. 14: 1132959.

- Song, S., Wang, Q., Xie, J., Dai, J., Ouyang, D., Huang, G., Guo, Y., Chen, C., Wu, M., Huang, T., Ruan, J., Cheng, X., Lin, X., He, Y., Rozhkova, E.A., Chen, Z., Yang, H. (2023). Dual-responsive turn-on T1 imaging-guided mild photothermia for precise apoptotic cancer therapy. *Adv Healthc Mater.* 28: e2301437.
- Spaepen, S., Vanderleyden, J. (2011). Auxin and plant-microbe interactions. *Cold Spring Harb Perspect Biol.* 3: a001438.
- Tang, A.D., Soulette, C.M., van Baren, M.J., Hart, K., Hrabeta-Robinson, E., Wu, C.J., Brooks, A.N. (2020). Full-length transcript characterization of SF3B1 mutation in chronic lymphocytic leukemia reveals downregulation of retained introns. *Nat Commun.* 11: 1438.
- Tang, J., Chen, S., Jia, G. (2023). Detection, regulation, and functions of RNA N^6 -methyladenosine modification in plants. *Plant Commun.* 4: 100546.
- Tian, S., Wu, N., Zhang, L., Wang, X. (2021). RNA N^6 -methyladenosine modification suppresses replication of rice black streaked dwarf virus and is associated with virus persistence in its insect vector. *Mol Plant Pathol.* 22: 1070-1081.
- Wang, L., Yang, C., Shan, Q., Zhao, M., Yu, J., Li, Y.F. (2023a). Transcriptome-wide profiling of mRNA N^6 -methyladenosine modification in rice panicles and flag leaves. *Genomics.* 115: 110542.
- Wang, X., Chen, Y., Liu, S., Fu, W., Zhuang, Y., Xu, J., Lou, Y., Baldwin, I.T., Li, R. (2023b). Functional dissection of rice jasmonate receptors involved in development and defense. *New Phytol.* 238: 2144-2158.
- Wang, X., Zhao, B.S., Roundtree, I.A., Lu, Z., Han, D., Ma, H., Weng, X., Chen, K., Shi, H., He, C. (2015). N^6 -methyladenosine modulates messenger RNA translation efficiency. *Cell.* 161: 1388-1399.
- Wang, Y., Du, F., Li, Y., Wang, J., Zhao, X., Li, Z., Xu, J., Wang, W., Fu, B. (2022). Global N^6 -methyladenosine profiling revealed the tissue-specific epitranscriptomic regulation of rice responses to salt stress. *Int J Mol Sci.* 23: pii: ijms23042091.
- Wang, Y., Wang, Y., Patel, H., Chen, J., Wang, J., Chen, Z.S., Wang, H. (2023c). Epigenetic modification of m⁶A regulator proteins in cancer. *Mol Cancer.* 22: 102.
- Wang, Y., Xiao, Y., Dong, S., Yu, Q., Jia, G. (2020). Antibody-free enzyme-assisted chemical approach for detection of N^6 -methyladenosine. *Nat Chem Biol.* 16: 896-903.
- Wang, Y., Zhang, L., Ren, H., Ma, L., Guo, J., Mao, D., Lu, Z., Lu, L., Yan, D. (2021). Role of Hakai in m⁶A modification pathway in *Drosophila*. *Nat Commun.* 12: 2159.
- Wei, L.H., Song, P., Wang, Y., Lu, Z., Tang, Q., Yu, Q., Xiao, Y., Zhang, X., Duan, H.C., Jia, G. (2018). The m⁶A reader ECT2 controls trichome morphology by affecting mRNA stability in Arabidopsis. *Plant Cell.* 30: 968-985.
- Xu, J., Wang, X., Zu, H., Zeng, X., Baldwin, I.T., Lou, Y., Li, R. (2021). Molecular dissection of rice phytohormone signaling involved in resistance to a piercing-sucking herbivore. *New Phytol.* 230: 1639-1652.
- Yahara, K., Suzuki, M., Hirabayashi, A., Suda, W., Hattori, M., Suzuki, Y., Okazaki, Y. (2021). Long-read metagenomics using PromethION uncovers oral bacteriophages and their interaction with host bacteria. *Nat Commun.* 12: 27.
- Yang, D.L., Yao, J., Mei, C.S., Tong, X.H., Zeng, L.J., Li, Q., Xiao, L.T., Sun, T.P., Li, J., Deng, X.W., Lee, C.M., Thomashow, M.F., Yang, Y., He, Z., He, S.Y. (2012). Plant hormone jasmonate prioritizes defense over growth by interfering with gibberellin signaling cascade. *Proc Natl Acad Sci U S A.* 109: E1192-1200.
- Yang, X., Wei, X., Yang, J., Du, T., Yin, C., Fu, B., Huang, M., Liang, J., Gong, P., Liu, S., Xie, W., Guo, Z., Wang, S., Wu, Q., Nauen, R., Zhou, X., Bass, C., Zhang, Y. (2021). Epitranscriptomic regulation of insecticide resistance. *Sci Adv.* 7: pii: 7/19/eabe5903.

Ye, G., Li, J., Yu, W., Xie, Z., Zheng, G., Liu, W., Wang, S., Cao, Q., Lin, J., Su, Z., Li, D., Che, Y., Fan, S., Wang, P., Wu, Y., Shen, H. (2023). ALKBH5 facilitates CYP1B1 mRNA degradation via m⁶A demethylation to alleviate MSC senescence and osteoarthritis progression. *Exp Mol Med.* 55: 1743-1756.

Yu, F., Qi, H., Gao, L., Luo, S., Njeri Damaris, R., Ke, Y., Wu, W., Yang, P. (2023). Identifying RNA modifications by direct RNA sequencing reveals complexity of epitranscriptomic dynamics in rice. *Genom Proteom Bioinf.* pii: S1672-0229(23)00034-7.

Zha, W., Li, C., Wu, Y., Chen, J., Li, S., Sun, M., Wu, B., Shi, S., Liu, K., Xu, H., Li, P., Liu, K., Yang, G., Chen, Z., Xu, D., Zhou, L., You, A. (2023). Single-cell RNA sequencing of leaf sheath cells reveals the mechanism of rice resistance to brown planthopper (*Nilaparvata lugens*). *Front Plant Sci.* 14: 1200014.

Zhang, K., Zhuang, X., Dong, Z., Xu, K., Chen, X., Liu, F., He, Z. (2021a). The dynamics of N⁶-methyladenine RNA modification in interactions between rice and plant viruses. *Genome Biol.* 22: 189.

Zhang, T.Y., Wang, Z.Q., Hu, H.C., Chen, Z.Q., Liu, P., Gao, S.Q., Zhang, F., He, L., Jin, P., Xu, M.Z., Chen, J.P., Yang, J. (2021b). Transcriptome-wide N⁶-methyladenosine (m⁶A) profiling of susceptible and resistant wheat varieties reveals the involvement of variety-specific m⁶A modification involved in virus-host interaction pathways. *Front Microbiol.* 12: 656302.

Zhou, L., Tang, R., Li, X., Tian, S., Li, B., Qin, G. (2021). N⁶-methyladenosine RNA modification regulates strawberry fruit ripening in an ABA-dependent manner. *Genome Biol.* 22: 168.

Supporting Information

Figure S1. Experimental flow chart of nanopore direct RNA sequencing.

Figure S2. Overall transcriptomic changes in rice in response to BPH infestation.

Figure S3. The overall m⁶A sites distribution along the mRNA in each group.

Figure S4. Histograms show the number of m⁶A methylation positions in un-infested and BPH-infested plants.

Figure S5. Differentiated m⁶A modification in BPH-infested rice plants.

Figure S6. Consensus motifs containing m⁶A methylation sites in BPH-infested and un-infested plants.

Figure S7. Euclidian distance coefficients among gene transcript profiles based on DRS analysis of two treatments.

Figure S8. Correlation analysis between m⁶A methylation and transcription abundance of target gene bodies in rice under BPH infestation.

Figure S9. Correlation analysis of m⁶A modification and differentially expressed transcripts in BPH-infested rice plants.

Figure S10. The number of gene bodies decreased along with the m⁶A modification sites increased.

Figure S11. GO and KEGG analyses of differentially m⁶A methylated genes in BPH-infested rice plants.

Figure S12. Expression analysis of SA pathway-related genes and SA quantification in BPH-infested rice.

Figure S13. RNA loading control that corresponding to the dot-blot analyses.

Table S1. Distribution of m⁶A modification sites on rice chromosomes in each treatment group.

Table S2. The number of m⁶A modification sites in each treatment group.

Table S3. Information of specific m⁶A methylation positions in NI-Nip vs. Nip comparison.

Table S4. Motifs of m⁶A modification sites in each treatment group.

Table S5. Transcripts Per kilobase of exon model per Million mapped reads (TPM) of all genes in each treatment group.

Table S6. Integrated analyses of m⁶A modification sites, m⁶A directions, transcriptome expression levels, and transcript regulatory direction.

Table S7. Detailed information of the m⁶A methylated genes appeared in enriched GO pathways under BPH infestation.

Table S8. Detailed information of the m⁶A methylated genes appeared in enriched KEGG pathways under BPH infestation.

Table S9. m⁶A modification profile of the main m⁶A modification machinery components.

Table S10. Analysis of m⁶A position and direction of the main m⁶A modification machinery components genes in Nip and NI-Nip treatment groups.

Table S11. m⁶A modification profile of the brown planthopper resistance-, cellulose and hemicellulose synthesis-related genes.

Table S12. Analysis of m⁶A position and direction of the BPH resistance genes in Nip and NI-Nip treatment groups.

Table S13. Analysis of m⁶A position and direction of the cellulose synthesis genes in Nip and NI-Nip treatment groups.

Table S14. Analysis of m⁶A position and direction of the hemicellulose synthesis genes in Nip and NI-Nip treatment groups.

Table S15. m⁶A modification profile of the JA- and SA-metabolism related genes.

Table S16. Analysis of m⁶A position and direction of the JA biosynthesis genes in Nip and NI-Nip treatment groups.

Table S17. Analysis of m⁶A position and direction of the JA response genes in Nip and NI-Nip treatment groups.

Table S18. Analysis of m⁶A position and direction of the SA biosynthesis genes in Nip and NI-Nip treatment groups.

Table S19. Analysis of m⁶A position and direction of the SA responsive genes in Nip and NI-Nip treatment groups.

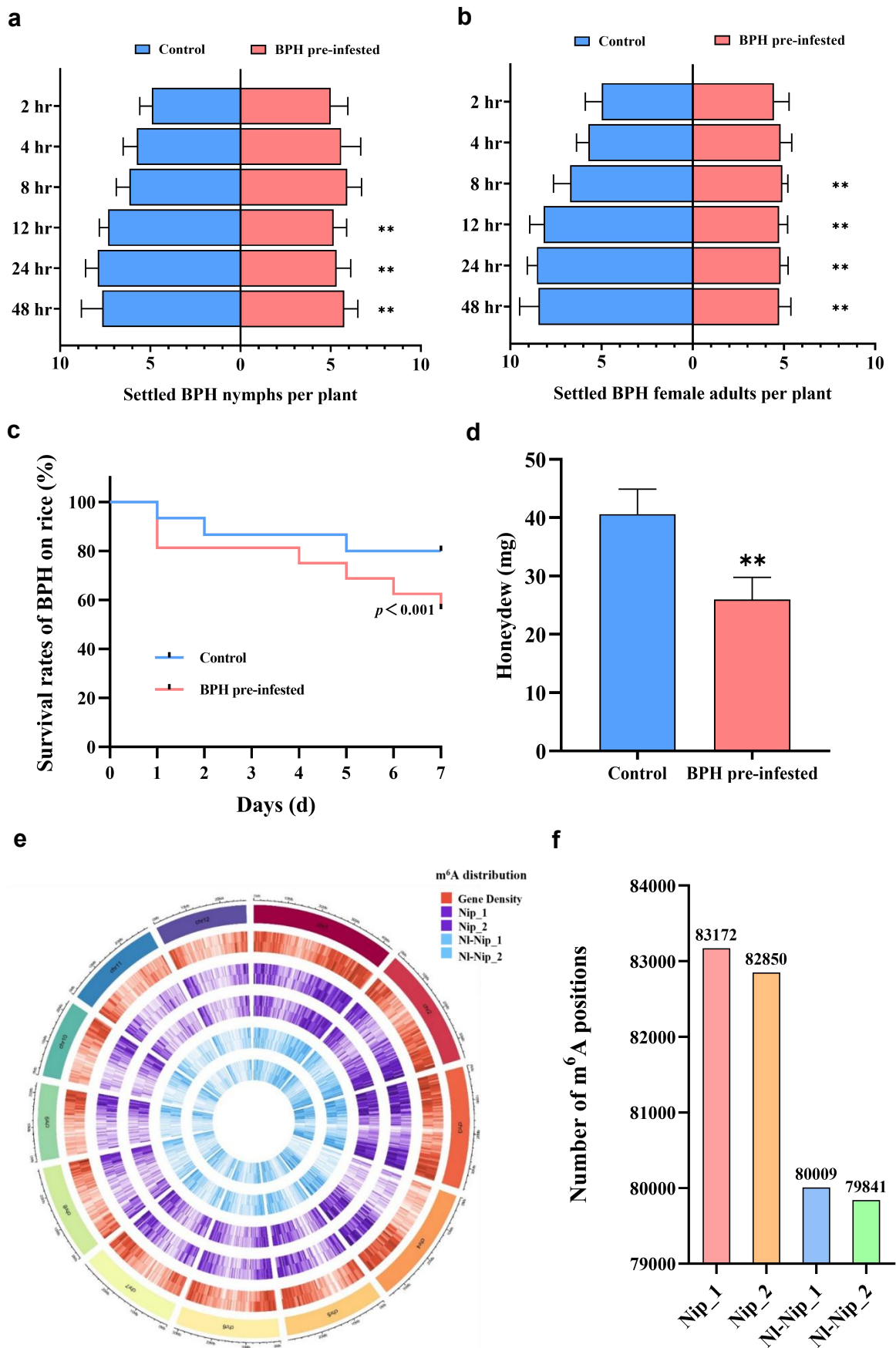
Table S20. m⁶A modification profile of rice growth-related genes.

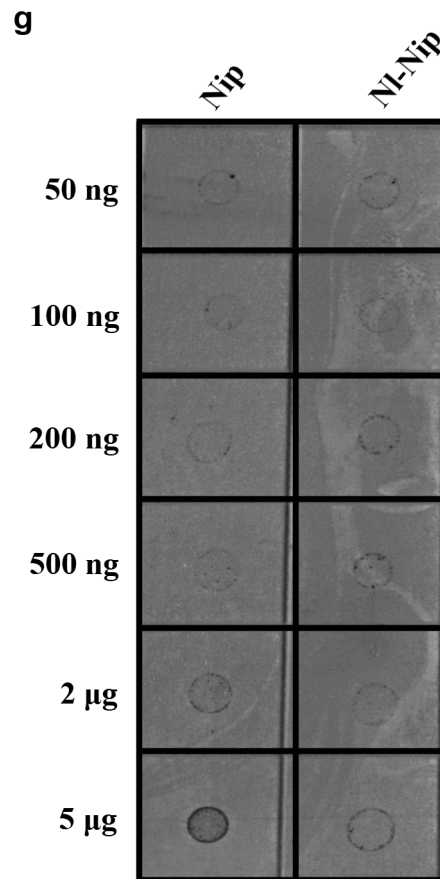
Table S21. Analysis of m⁶A position and direction of auxin-related genes in Nip and NI-Nip treatment groups.

Table S22. Analysis of m⁶A position and direction of gibberellin-related genes in Nip and NI-Nip treatment groups.

Table S23. Primers used in RT-qPCR qualification of the candidate genes.

1 Figure Legends





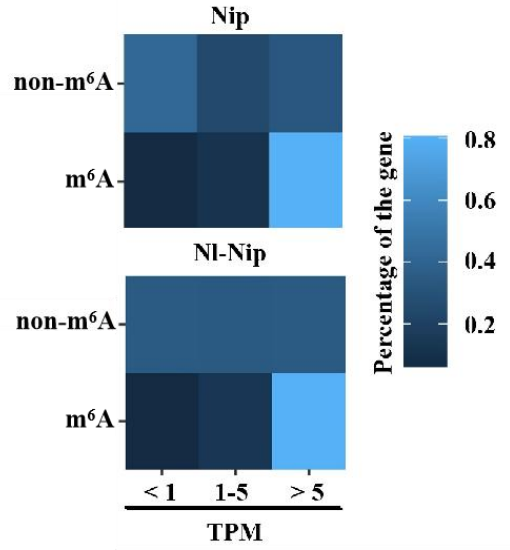
3

4 **FIGURE 1** The increase of rice resistance infested by BPH gravid females and its
5 overall m⁶A modification

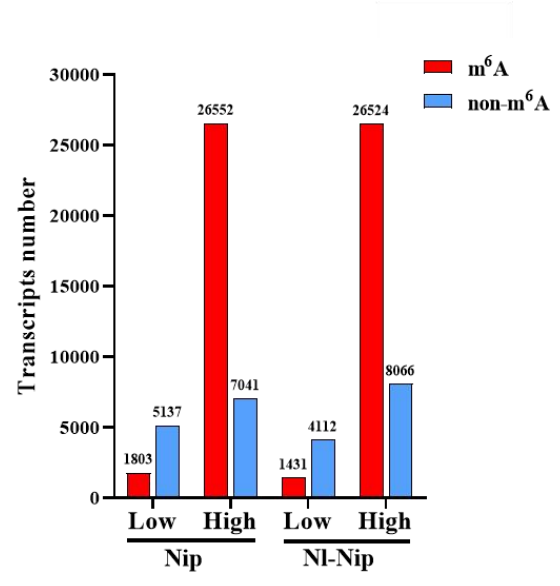
6 (a, b) Mean number of BPH nymphs (a) and female adults (b) per plant for plant pairs
7 ($n = 12$; BPH pre-infested rice vs control rice). Fifteen fourth instar nymphs and
8 gravid female adults were released for each replicate. (c) Mean survival rates of
9 nymphs across time ($n = 8$). (d) Mean amount of honeydew excreted by a female
10 adult 24 h after the start of the experiment ($n = 18$). All choice and no-choice assays
11 were performed after 24 h of continuous gravid females infestation on rice leaf
12 sheaths (BPH pre-infested), whereas untreated rice plants were used as the controls. (e)
13 Circo plots of m⁶A methylome in rice plants. The six rings from outside to inside
14 show the genomic positions (1st ring), gene density (2nd ring), m⁶A methylome density
15 of control rice plants (3rd and 4th rings), m⁶A methylome density of BPH-infested
16 plants (5th and 6th rings). The outer loop of each ring (3rd–6th rings) represents the

17 plus-strand of the genome and the inner loop represents the minus-strand. (f)
18 Histograms showing the number of m⁶A methylation positions in control (Nip_1,
19 Nip_2) and BPH-infested Nipponbare plants (NI-Nip_1, NI-Nip_2). The Y-axis
20 represents the total position number and X-axis represents the two treatments. Two
21 biological replicates were used for each treatment. (g) Dot-blot analysis of m⁶A levels
22 in total RNA extracted from rice samples using the specific anti-m⁶A antibodies. Error
23 bars represent standard errors. Asterisks indicate significant differences (** $p < 0.01$;
24 ns, no significant difference; Student's *t*-test). m⁶A, N⁶-methyladenosine; BPH, brown
25 planthopper; Nip, control Nipponbare rice; NI-Nip, BPH-infested Nipponbare rice.

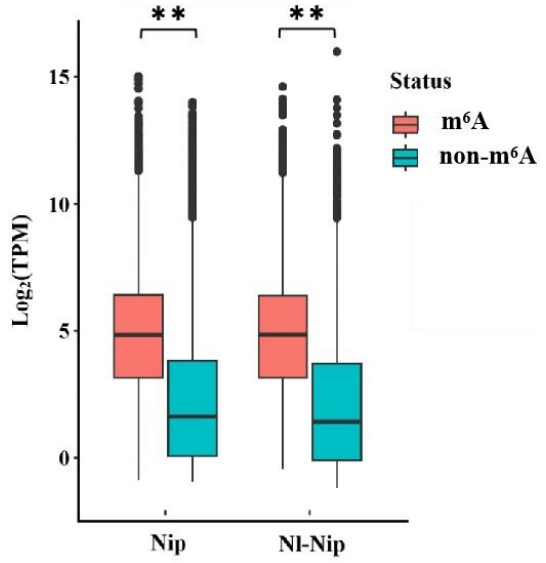
a



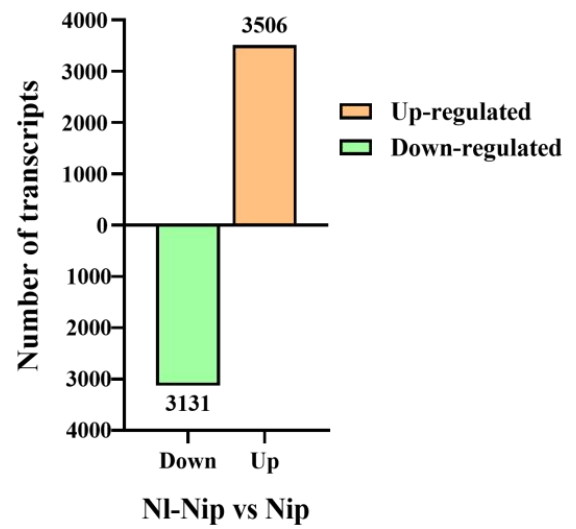
b

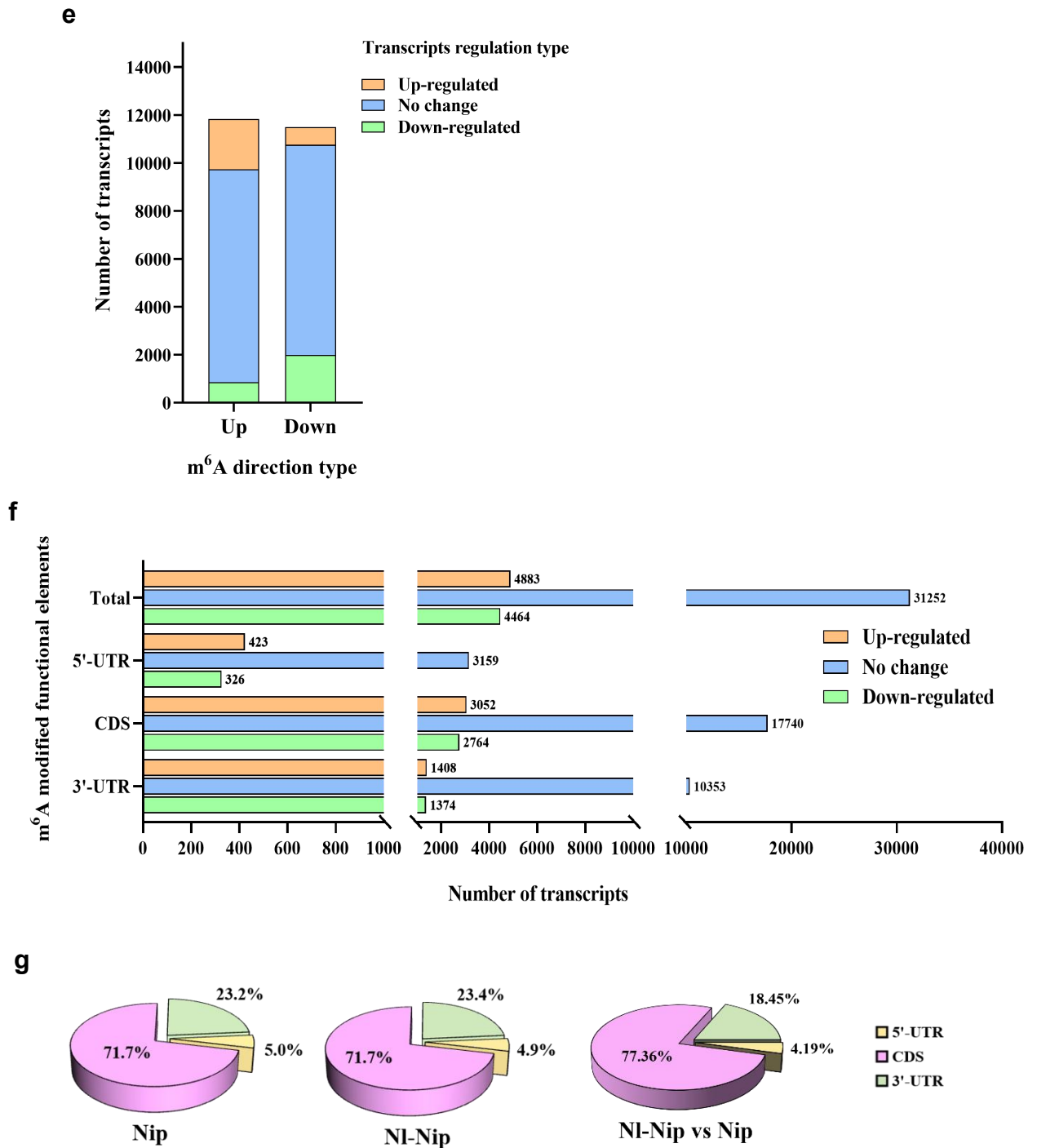


c



d

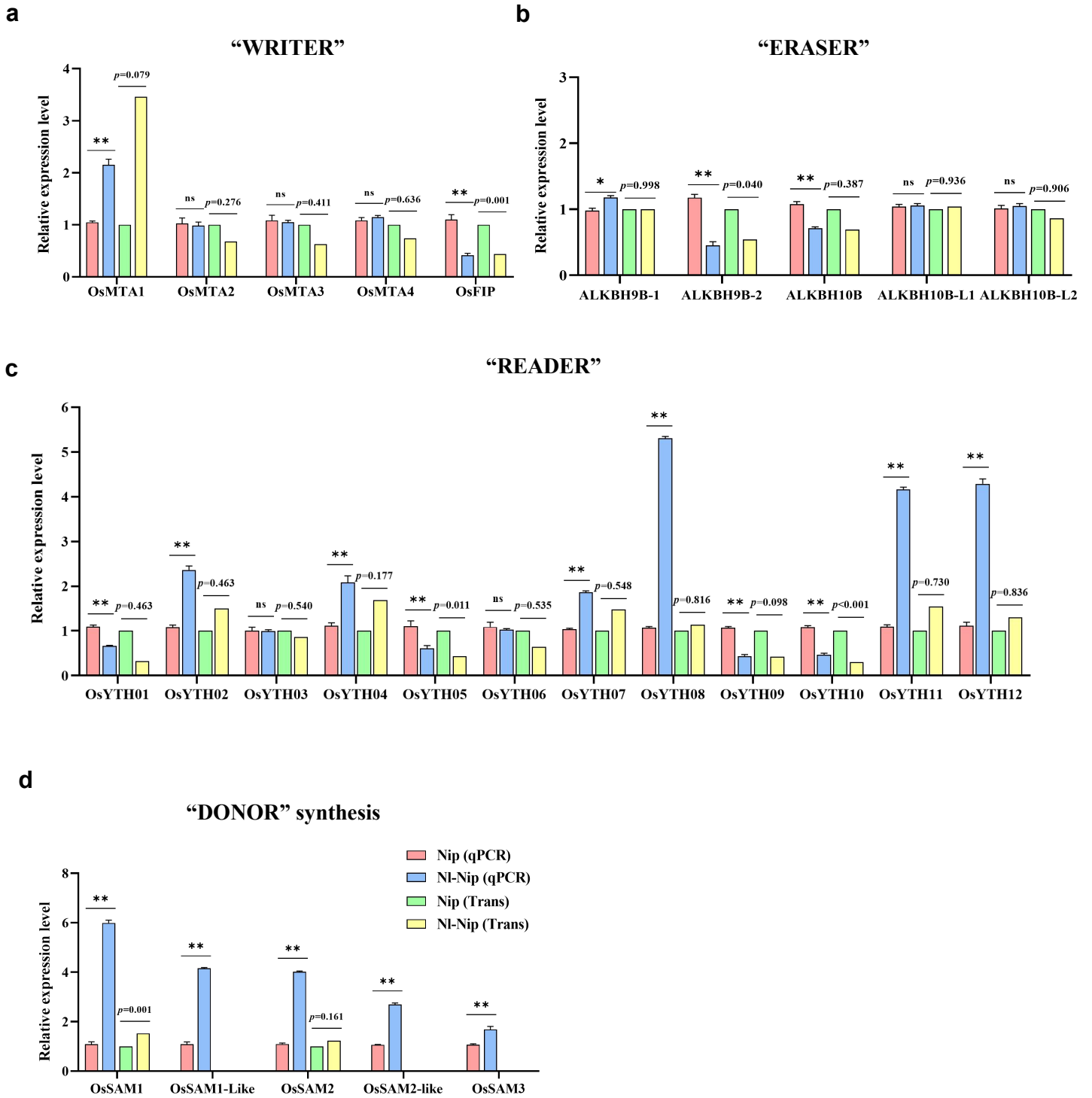




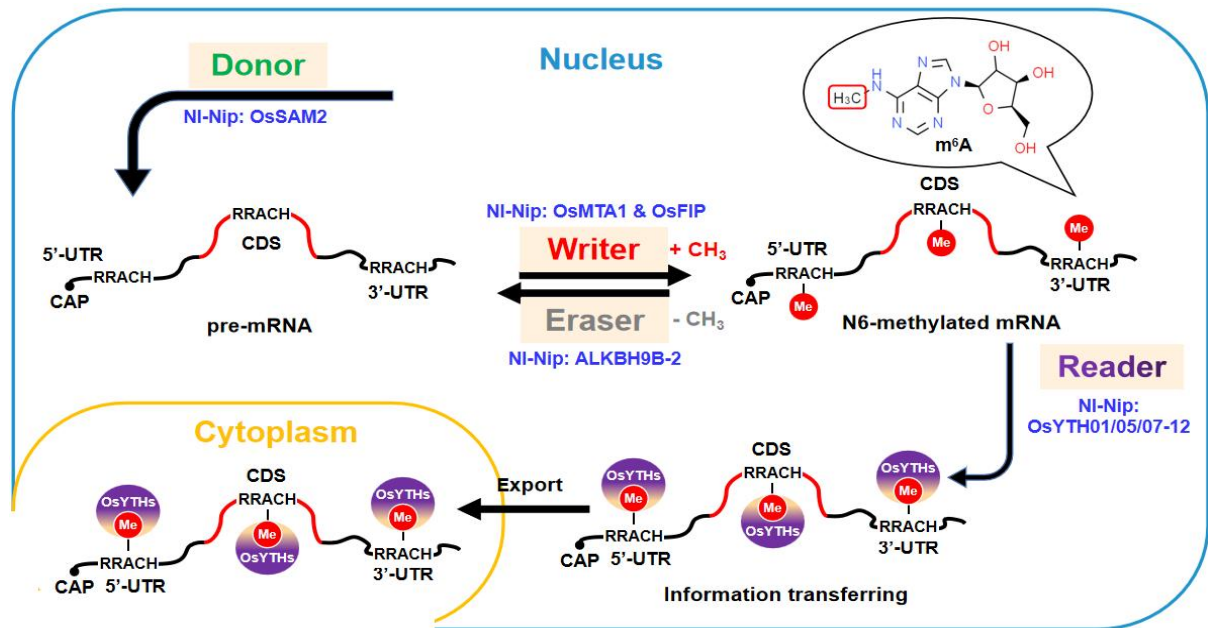
27 **FIGURE 2** Integrated analyses of the relationship between transcripts regulation and
 28 m⁶A modification
 29 (a) The percentage of rice m⁶A methylated and un-methylated genes at defined TPM
 30 (Transcripts Per kilobase of exon model per Million mapped reads) levels (< 1, 1–5,
 31 and > 5). Color densities indicate different percentages of genes in a category. (b)

32 Comparisons of the number of non-m⁶A methylated genes and m⁶A methylated genes
33 in their gene bodies with high (High: TPM > 1) and lower (Low: TPM < 1) expression
34 levels in each treatment. (c) Box plot comparing TPM expression levels between
35 non-m⁶A and m⁶A methylated genes in each treatment. Asterisks indicate significant
36 differences (** $p < 0.01$; Student's t -test). (d) Histograms showing the number of
37 significantly up- and down-regulated transcripts that contain m⁶A modifications in
38 NI-Nip vs. Nip comparison group. (e) Stack diagram of the relationship between the
39 m⁶A methylation differential types and the corresponding transcripts differential types
40 in NI-Nip vs. Nip comparison group. The Y-axis represents transcripts of different
41 regulation types as well as their numbers, and X-axis shows the up- and
42 down-directed m⁶A methylated transcripts in NI-Nip vs. Nip group. (f) Widely
43 integrated analyses of the relationship between the transcript expression levels and
44 m⁶A methylated functional elements using the m⁶A modified transcripts in NI-Nip vs.
45 Nip group. The Y-axis represents the different gene structure of m⁶A modification
46 regions; X-axis shows the number of transcripts with different regulatory types. (g)
47 Percentages of each gene body in differentially m⁶A-methylated genes in control Nip,
48 NI-Nip, as well as in NI-Nip vs. Nip group. m⁶A, N⁶-methyladenosine; BPH, brown
49 planthopper; Nip, control Nipponbare rice sample; NI-Nip, BPH-infested Nipponbare
50 rice sample.

51
52



e



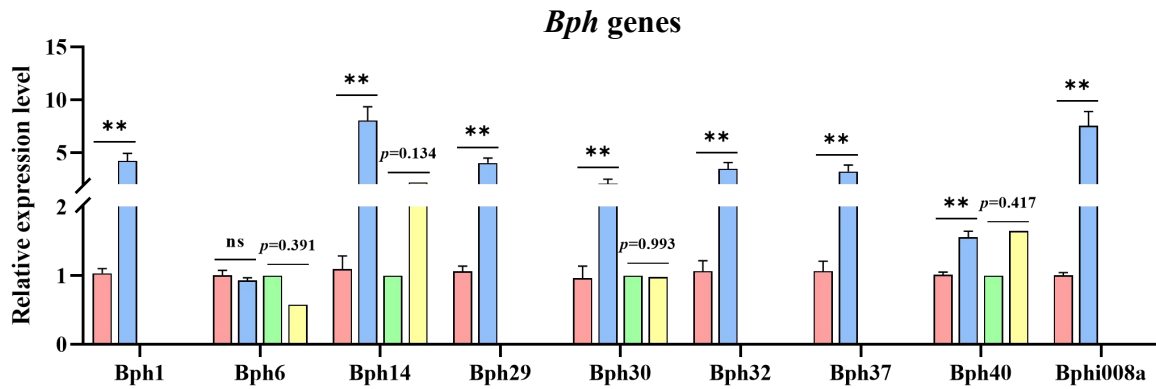
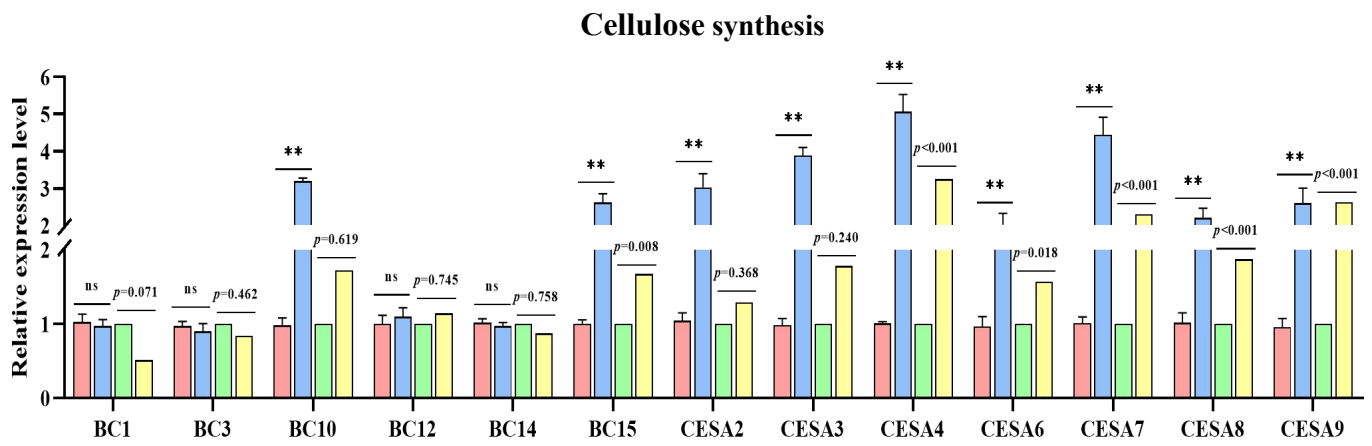
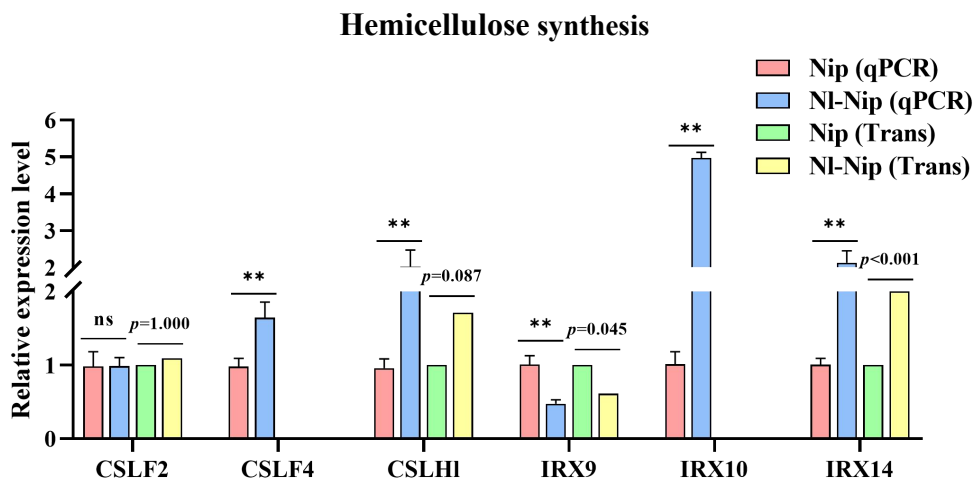
53

54

55 **FIGURE 3** Relative expression levels of rice genes involved in m⁶A methylation
 56 machinery under BPH infestation

57 (a–d) RT-qPCR and transcriptome analysis of the relative expression of 5 “WRITER”
 58 genes (a), 5 “ERASER” genes (b), 12 “READER” genes (c), and 5 methyl “DONOR”
 59 synthesis genes (d) in Nip and NI-Nip plants. Some undetected transcriptome data
 60 indicated the absence of m⁶A methylation sites in the transcript. Error bars represent
 61 standard errors. Asterisks indicate significant differences (* $p < 0.05$; ** $p < 0.01$; ns,
 62 no significant difference; Student’s t -test). (e) Rice m⁶A methylation pathways and
 63 related genes upon BPH infestation. Blue letters indicate differentially expressed
 64 transcripts containing differentially directed m⁶A methylation with the same
 65 regulatory trend. *OsSAM2* means that *OsSAM2* was up-regulated and showed
 66 up-directed m⁶A methylation in NI-Nip compared with in Nip plants. *OsFIP* indicates
 67 that *OsFIP* was down-regulated and also showed down-directed m⁶A methylation in
 68 NI-Nip compared with in Nip plants. The differentially expressed transcripts showed a
 69 transcriptional expression fold change of < 0.5 or > 2 ($p < 0.05$), along with a
 70 significant m⁶A methylation direction ($p < 0.05$), and $|\text{meth diff}| > 10$. m⁶A,

- 71 N^6 -methyladenosine; BPH, brown planthopper; Nip, control Nipponbare rice; NI-Nip,
72 BPH-infested Nipponbare rice.

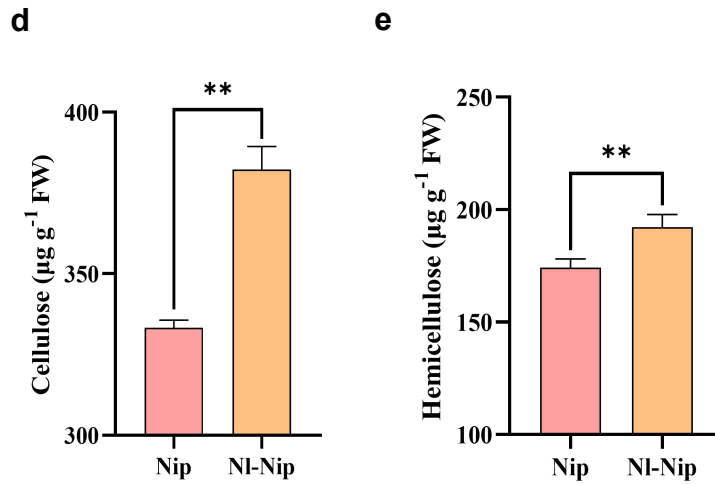
a**b****c**

74

75

76

77

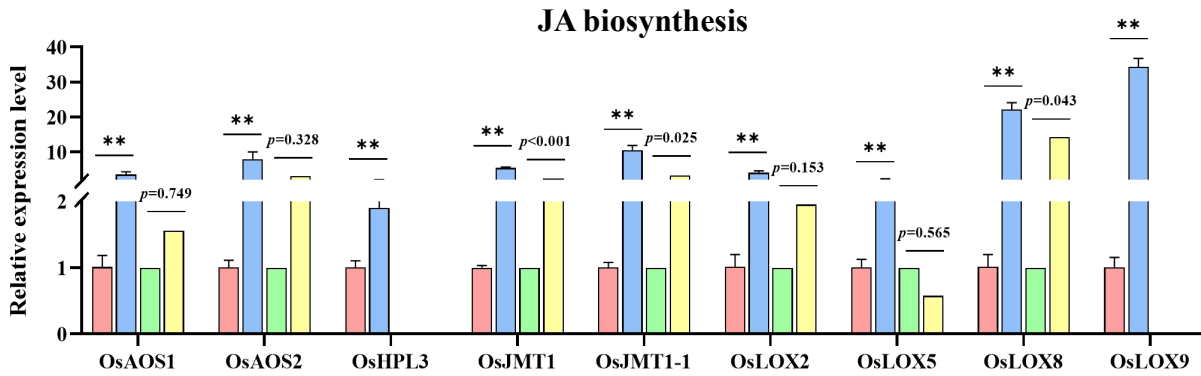


78

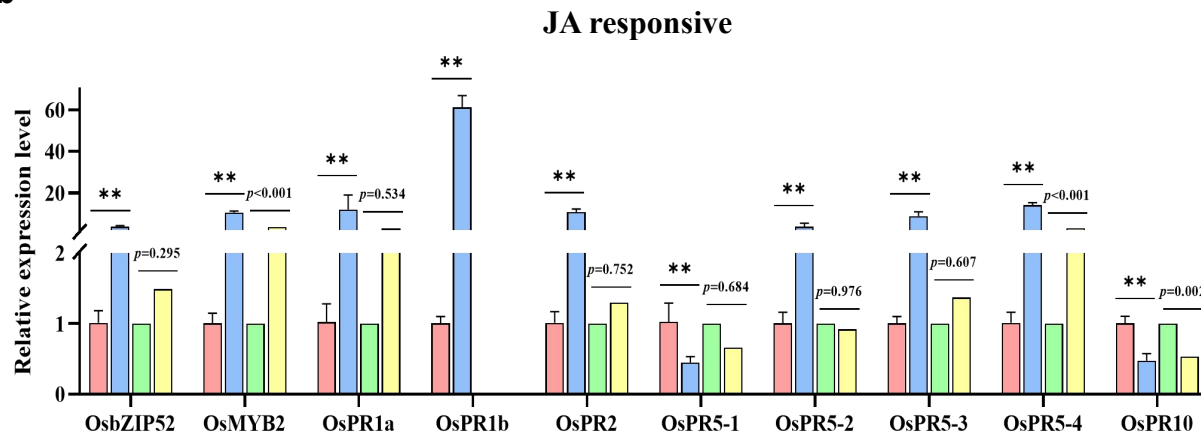
79 **FIGURE 4** The BPH infestation activated cellulose- and hemicellulose-synthesis
80 pathways

81 (a–c) RT-qPCR and transcriptome analysis of the relative expression of 9 *Bph* genes
82 (a), 13 cellulose synthesis genes (b), and 6 hemicellulose synthesis genes (c) in Nip
83 and NI-Nip plants. Some undetected transcriptome data indicated the absence of m⁶A
84 methylation sites in the transcript. (d, e) Mean levels ($n = 6$) of cellulose (d) and
85 hemicellulose (e) in Nip and NI-Nip plants. Error bars represent standard errors.
86 Asterisks indicate significant differences (** $p < 0.01$; ns, no significant difference;
87 Student's *t*-test). Nip, control Nipponbare rice; NI-Nip, BPH-infested Nipponbare rice;
88 FW, fresh weight.

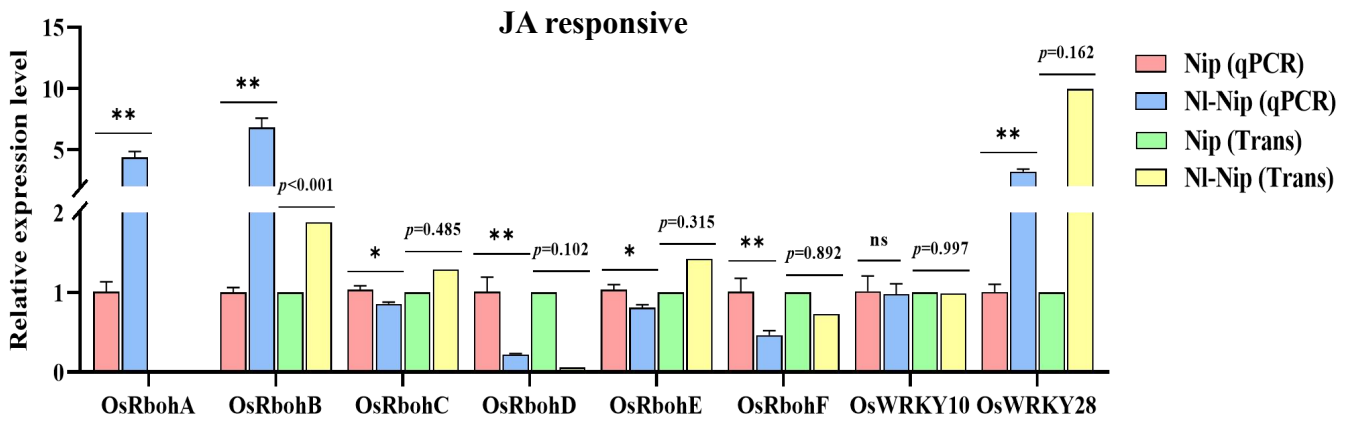
a



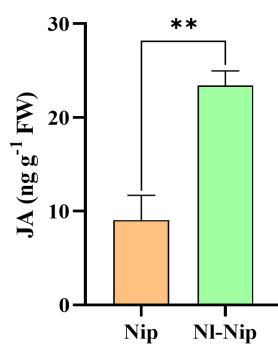
b



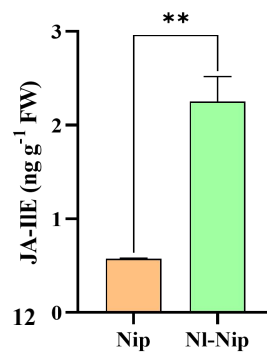
c



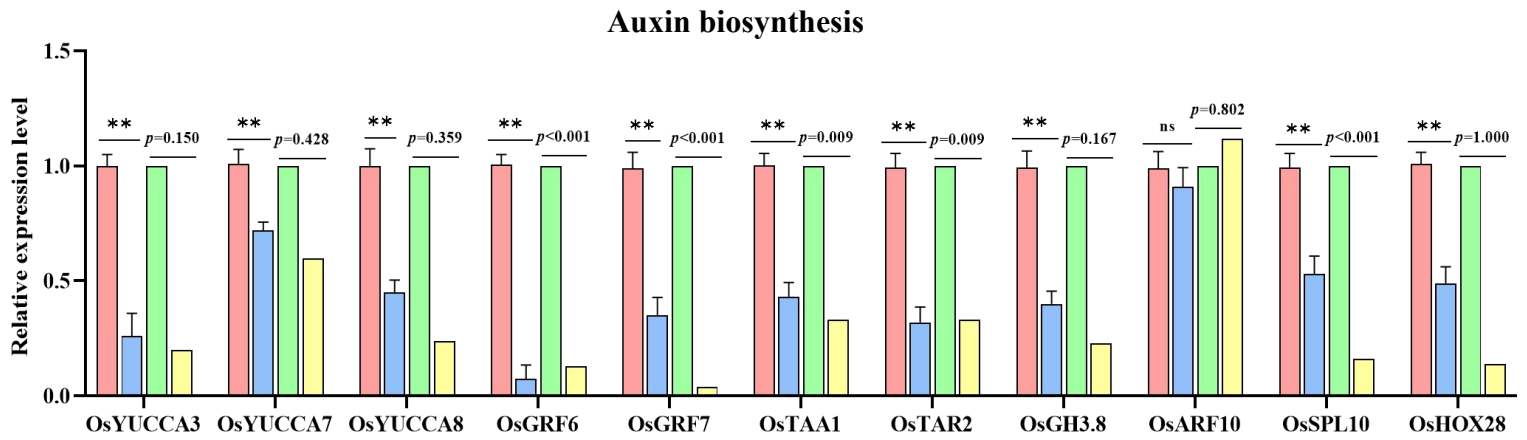
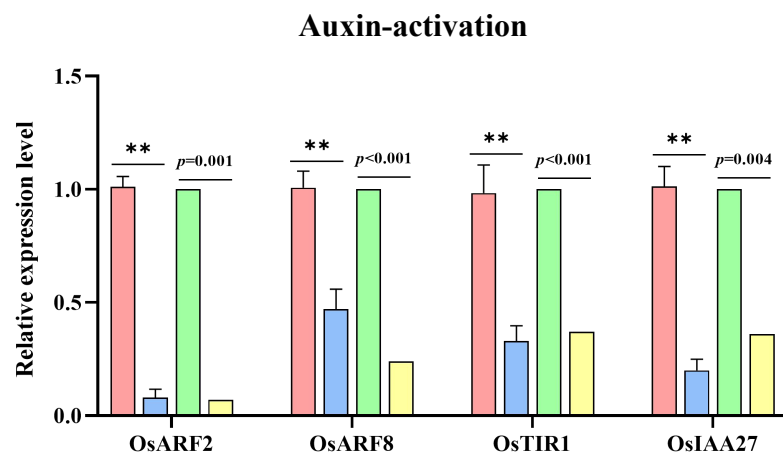
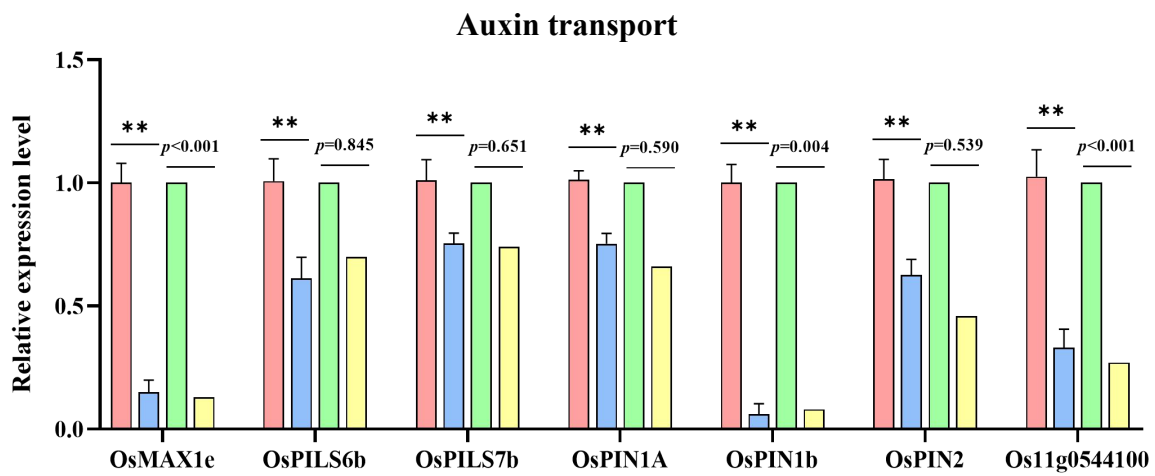
d



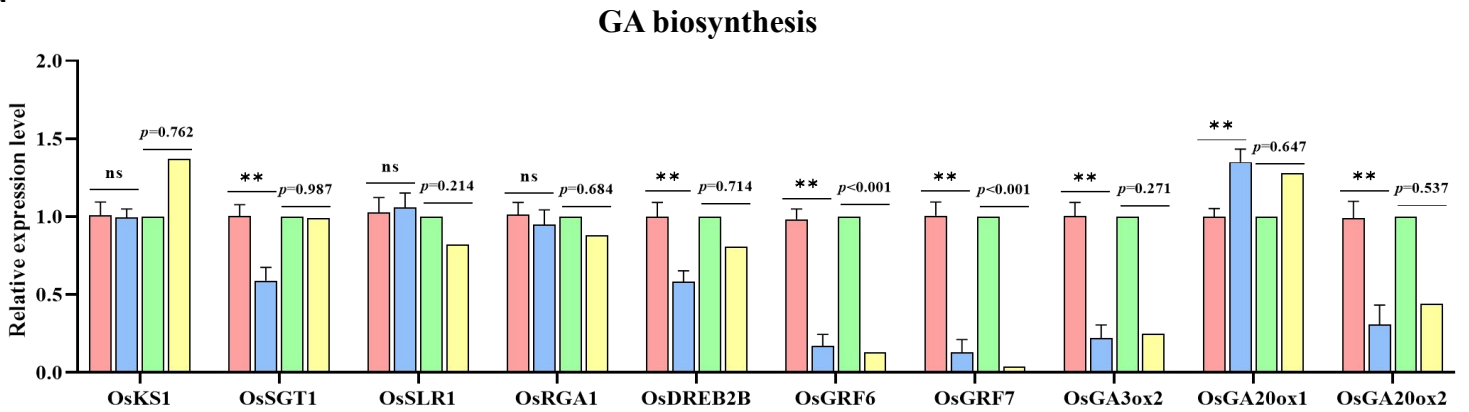
e



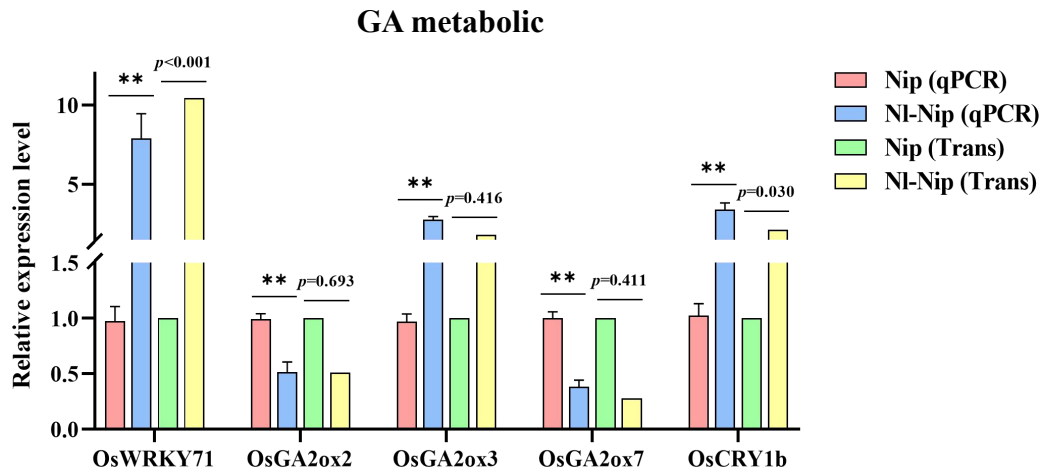
91 **FIGURE 5** Jasmonic acid biosynthesis and responsive pathways were activated in
92 BPH-infested rice plants
93 (a–c) RT-qPCR and transcriptome analysis of the relative expression of 9 JA
94 biosynthesis-related genes (a), and 18 JA responsive genes (b, c) in Nip and NI-Nip
95 plants. Some undetected transcriptome data indicated the absence of m⁶A methylation
96 sites in the transcript. (d, e) Mean levels ($n = 6$) of JA (d), and jasmonoyl-isoleucine
97 (JA-ILE) (e) in Nip and NI-Nip plants. Error bars represent standard errors. Asterisks
98 indicate significant differences (* $p < 0.05$; ** $p < 0.01$; ns, no significant difference;
99 Student's t -test). Nip, control Nipponbare rice; NI-Nip, BPH-infested Nipponbare rice;
100 FW, fresh weight.

a**b****c**

d



e



103

104 **FIGURE 6** Auxin pathways and gibberellic acid biosynthesis process were activated

105 in BPH-infested rice plants

106 (a–e) RT-qPCR and transcriptome analysis of the relative expression of Auxin

107 biosynthetic process (a), Auxin-activated signaling pathway (b), Auxin

108 transport-related (c), gibberellic acid (GA) biosynthetic (d), and GA metabolic (e)

109 genes in Nip and NI-Nip plants. Error bars represent standard errors. Asterisks

110 indicate significant differences (** $p < 0.01$; ns, no significant difference; Student's111 *t*-test). BPH, brown planthopper; Nip, control Nipponbare rice; NI-Nip, BPH-infested

112 Nipponbare rice.

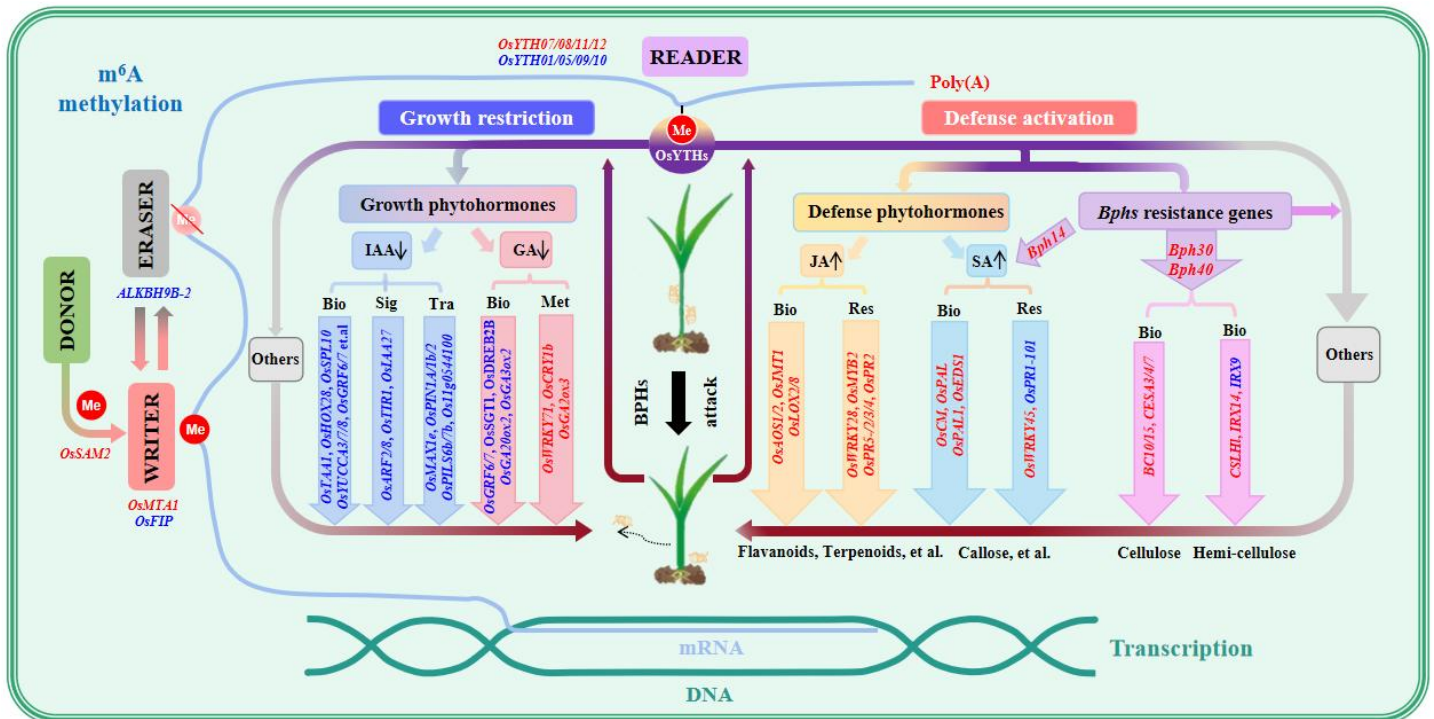


FIGURE 7 Proposed model of the rice m⁶A RNA methylation modulation in key defense and growth pathways regulated by BPH infestation

The genes highlighted in red denote both transcriptional up-regulated ($p < 0.05$) and up-directed m⁶A modification ($p < 0.05$ and $|\text{meth diff}| > 10$). The number of up-directed m⁶A sites occurring on the target pathway in NI-Nip vs. Nip group was less than that of down-directed m⁶A sites. Genes highlighted in blue represent both transcriptional down-regulated ($p < 0.05$) and down-directed m⁶A modification; the number of down-directed m⁶A sites occurring on the target pathway in NI-Nip vs. Nip group was less than that of up-directed m⁶A sites ($p < 0.05$ and $|\text{meth diff}| > 10$). The upward arrows indicate increased phytohormones content, and downward arrows indicate decreased phytohormones content. Bio, biosynthetic process; Sig, activated signaling process; Tra, transport process; Met, metabolic process; Res, responsive process; m⁶A, N⁶-methyladenosine; BPH, brown planthopper; Nip, control Nipponbare rice; NI-Nip, BPH-infested Nipponbare rice.